

# 1 Flood risk assessment for Indian sub-continental river basins

2 Urmin Vegad<sup>1</sup>, Yadu Pokhrel<sup>2</sup>, and Vimal Mishra<sup>1,3\*</sup>

3  
4 <sup>1</sup>Civil Engineering, Indian Institute of Technology (IIT) Gandhinagar

5 <sup>2</sup>Department of Civil and Environmental Engineering, Michigan State University, East Lansing, Michigan, USA

6 <sup>3</sup>Earth Sciences, Indian Institute of Technology (IIT) Gandhinagar

7 \*Corresponding author: vmishra@iitgn.ac.in

## 8 Abstract

9 Floods are among India's most frequently occurring natural disasters, which disrupt all aspects of socio-economic  
10 well-being. A large population is affected by floods during almost every summer monsoon season in India, leaving  
11 its footprint through human mortality, migration, and damage to agriculture and infrastructure. Despite the  
12 massive imprints of floods, sub-basin level flood risk assessment is still in its infancy and requires advancements.  
13 Using hydrological and hydrodynamical models, we reconstructed sub-basin level observed floods for the 1901-  
14 2020 period. Our modelling framework includes the influence of 51 major reservoirs that affect flow variability  
15 and flood inundation. Sub-basins in the Ganga and Brahmaputra River basins witnessed substantial flood  
16 inundation extent during the worst flood in the observational record. Major floods in the sub-basins of the Ganga  
17 and Brahmaputra occur during the late summer monsoon season (August-September). Beas, Brahmani, upper  
18 Satluj, Upper Godavari, Middle and Lower Krishna, and Vashishti sub-basins are among the most influenced by  
19 the dams, while Beas, Brahmani, Ravi, and Lower Satluj are among the most impacted by floods and the presence  
20 of dams. Bhagirathi, Gandak, Kosi, lower Brahmaputra, and Ghaghara are India's sub-basins with the highest  
21 flood risk. Our findings have implications for flood risk assessment and mitigation in India.

## 22 1. Introduction

23 Flood risk to both natural and human systems is projected to increase due to climate change (IPCC, 2014, 2022).  
24 Extreme weather and climate extremes have increased under warming climate, leading to an increased frequency  
25 of natural hazards like floods, droughts, heat waves, cyclones, and heavy rains. Hydroclimatic extremes affect  
26 humans and infrastructure (Eidsvig et al., 2017; Peduzzi et al., 2009). Due to high vulnerability and lower adaptive  
27 capacity, developing countries are often the most impacted by extreme weather events. Further, developing  
28 countries usually take longer to recover from the hazards due to low climate resilience. Globally, floods are among  
29 the most devastating natural hazards (Ghosh & Kar, 2018). Among all flood types, riverine floods occur most  
30 frequently (Kimuli et al., 2021) and often cause substantial damage to agriculture and infrastructure. A  
31 considerable fraction of the population and infrastructure are exposed to flooding, which will also increase due to  
32 the projected increase in the magnitude and frequency of floods (Winsemius et al., 2018).

33 The increase in flood magnitude due to the warming climate has resulted in considerable economic losses (C. M.  
34 R. Mateo et al., 2014; Willner et al., 2018). The total financial loss will likely increase by 17% in the next 20 years  
35 due to climate change (Willner et al., 2018). Besides agriculture, floods significantly affect the built environment  
36 and transportation infrastructure (Kalantari et al., 2014). For instance, more than 7% of road and railway assets

37 globally are exposed to a 100-year return period flood (Koks et al., 2019). In Asia, about 75% of the population  
38 is exposed to riverine floods (Varis et al., 2022). India falls among the top ten most flood-affected countries in  
39 Asia and the Pacific (Kimuli et al., 2021). In addition, India is also among the top-ten countries that experienced  
40 the highest human mortality due to floods. Considerable population exposure, climate change, and rapid growth  
41 and development in flood-prone areas contribute to increased losses from floods.

42 In India, state administration takes decisions to mitigate floods while the central government provides financial  
43 aid under severe conditions (Jain et al., 2017). The state authorities develop action plans to minimize flood  
44 damage. Therefore, identifying the regions with higher flood risk is essential for planning and mitigation. Flood  
45 impacts can be quantified according to the affected population, gross domestic product (GDP), and agricultural  
46 practices (Ward et al., 2013). The flood risk assessment framework suggested by the Intergovernmental Panel on  
47 Climate Change (IPCC) has been extensively applied at the regional and global scales (Allen et al., 2016; IPCC,  
48 2014; Roy et al., 2021). The risk can be quantified as a function of vulnerability, hazard, and exposure (IPCC,  
49 2014). To control the risk, reducing vulnerability is considered a short to the mid-term goal (V. Mishra et al.,  
50 2022), while reducing hazards and exposure are long-term goals (Birkmann & Welle, 2015). Flood risk  
51 assessment can assist in identifying the regions at high risk due to higher vulnerability, hazard, and exposure,  
52 which can be used for developing a framework, methodology, and guidelines for flood mitigation and damage  
53 assessment.

54 A flood risk assessment performed on a global scale may not help in identifying the flood risk-prone regions at a  
55 country scale due to the coarser spatial resolution (Bernhofen et al., 2022). Due to complex geomorphological  
56 characteristics and diverse climatic conditions, India is considered a relatively high flood-risk region (Hochrainer-  
57 Stigler et al., 2021). Therefore, estimating flood risk on a finer scale (e.g. sub-basin level) is essential for reliable  
58 flood risk assessment. There have been studies on regional or river basin scales (Allen et al., 2016; Ghosh &  
59 Kar, 2018; Roy et al., 2021); however, those do not provide flood risk at a sub-basin scale in India. In addition,  
60 the impact assessment of floods on transport infrastructure (rail and road infrastructure) still needs to be improved  
61 in the country (Pathak et al., 2020; P. Singh et al., 2018). In addition, the role of dams and reservoirs in the flood  
62 risk assessment should be addressed (Hirabayashi et al., 2013; Yamazaki et al., 2018). Dams and reservoirs  
63 considerably influence streamflow variability and can attenuate flood peaks (Dang et al., 2019; Vu et al., 2022;  
64 Zajac et al., 2017). In contrast, dam operations and decisions can also worsen the flood situation in the downstream  
65 regions. For instance, recent flooding in Kerala and Chennai was partly attributed to reservoir operations (V.  
66 Mishra & Shah, 2018). India has more than 5300 large dams regulating river flow (National Register of Large  
67 Dams (NRLD), 2019), affecting ecosystems, natural resources, and livelihoods (Acreman, 2000). Reservoirs  
68 impact flow regulation, magnitude, timing, and extent of flooding in the downstream regions. Therefore, flood  
69 risk assessment without considering the role of reservoirs can be inappropriate in the basins that are highly affected  
70 by the presence of dams.

71 We use the H08 (Hanasaki et al., 2018) global hydrological model combined with the CaMa-Flood (Yamazaki et  
72 al., 2011) model for the sub-basin level flood risk assessment in India considering the role of reservoirs. The  
73 CaMa-Flood model combined with the H08 model has been used for several river basins globally (Boulange et  
74 al., 2021; C. M. R. Mateo et al., 2013). The CaMa-Flood model performs well in simulating flood dynamics

75 (Chaudhari and Pokhrel, 2022; H. Dang et al., 2022; Gaur & Gaur, 2018; Hirabayashi et al., 2013, 2021;  
76 Yamazaki et al., 2018; Yang et al., 2019). The CaMa-Flood model takes runoff as input simulated from any  
77 hydrological model and can simulate flood depth and inundation. In India, almost all the major rivers are  
78 influenced by reservoirs (Lehner et al., 2011). Therefore, the major scientific questions that we address are: 1)  
79 How does the flood risk vary at the sub-basin scale in India for the observed worst floods that occurred during the  
80 1901-2020 period? 2) Which are the sub-basins where the presence of reservoirs considerably influences the flood  
81 risk? To address these questions, we use long-term observations (1901-2020) from India Meteorological  
82 Department (IMD) along with a hydrological modelling framework.

## 83 **2. Data and Methods**

### 84 **2.1 Datasets**

85 We used observed gridded precipitation (Pai et al., 2014) and daily maximum and minimum temperatures  
86 (Srivastava et al., 2009) from India Meteorological Department (IMD). We obtained gridded daily precipitation  
87 at 0.25° from IMD for the 1901-2020 period that was developed using station-based rainfall observations from  
88 more than 6900 gauge stations (Pai et al., 2014). The gridded rainfall product has been widely used for  
89 hydrological studies (Kushwaha et al., 2021; Shah & Mishra, 2016) and it captures the key features of the  
90 summer monsoon variability and orographic rainfall over the western Ghats and foothills of the Himalayas. We  
91 obtained daily 1° gridded maximum and minimum temperatures from IMD (Srivastava et al., 2009). The gridded  
92 temperature dataset is developed using observations from 395 stations located across India. Bilinear interpolation  
93 was used to convert the 1° gridded temperature to 0.25° resolution to make it consistent with the gridded  
94 precipitation. For the regions outside India, we obtained observational meteorological datasets (rainfall and  
95 temperature) at 0.25 degrees from Princeton University (Sheffield et al., 2006). Gridded datasets from Sheffield  
96 et al. (2006) compare well against the IMD observations and have been used in hydrological applications in India  
97 (Shah & Mishra, 2016).

98 Observed daily streamflow at gauge stations and reservoir live storage were obtained from India Water Resources  
99 Information System (India-WRIS). We considered the influence of 51 major reservoirs located in different river  
100 basins to examine the impact of reservoirs on floods using the CaMa-Flood model (Figure S1). The information  
101 of dams was obtained from the National Register of Large Dams (NRLD) [Table S1]. We used the Global Surface  
102 Water (GSW) extent to estimate flood occurrences at a monthly timescale (Pekel et al., 2016). Simulated flood  
103 occurrences during the period of the GSW database (1985-2020) were used to validate the performance of the  
104 hydrological model in simulating flood extent (Pekel et al., 2016). In addition, we obtained reported flood details  
105 from the Emergency Events Database (EM-DAT, <http://www.emdat.be/>) and Dartmouth Flood Observatory  
106 (DFO, <http://floodobservatory.colorado.edu/>). EM-DAT is developed by the Centre for Research on the  
107 Epidemiology of Disasters (CRED), while the University of Colorado manages DFO. We used population data  
108 from Global Human Settlement Layers (GHLS) to estimate flood exposure. Finally, we used roadway and railway  
109 network data to assess the impact of floods on the infrastructure.

### 110 **2.2 H08-CaMa-Flood combined model**

111 We used the H08 (Hanasaki et al., 2018) global hydrological model to simulate hydrological variables. The H08  
112 is a distributed global water resources model comprising six sub-models: land surface hydrology, river routing,  
113 reservoir operation, crop growth, environmental flow, and water abstraction. The model estimates baseflow using  
114 a leaky bucket method, while runoff is calculated based on saturation excess non-linear flow (Hanasaki et al.,  
115 2008). The H08 model can be run separately or combined with any hydrodynamic model to perform flow routing.  
116 The H08 model uses precipitation, air temperature, short and longwave radiations, wind speed, surface pressure,  
117 and specific humidity as input meteorological forcing. Soil parameters for the H08 model were obtained from  
118 Harmonized World Soil Database (HWSD). We forced the H08 model with the input meteorological forcing at  
119 0.25° spatial and daily temporal resolution. We combined the H08 land surface model with the CaMa-Flood  
120 model. The CaMa-Flood model has been previously combined with the H08 model to obtain flood inundation  
121 estimates (C. M. Mateo et al., 2014).

122 The CaMa-Flood (version 4.1) is a hydrodynamic model (Yamazaki et al., 2011), which simulates river-floodplain  
123 dynamics (Yamazaki et al., 2013). The CaMa-Flood model has been extensively used for better performance in  
124 simulating discharge and flood peaks (Zhao et al., 2017). The CaMa-Flood model considers the role of dams and  
125 reservoirs for streamflow and flood inundation simulations (Chaudhari & Pokhrel, 2022; C. M. Mateo et al.,  
126 2014; Pokhrel et al., 2018). We ran the CaMa-Flood model at a finer spatial resolution (0.1°) using the H08-  
127 simulated runoff (0.25°) as input. We calibrated the combined model (H08 and CaMa-Flood) for India's eighteen  
128 major river basins for at least one gauge station each, considering the influence of 51 major dams. The gauge  
129 stations were selected in the farthest downstream of the river basin based on the availability of observed  
130 streamflow. The influence of reservoir operations was simulated using the CaMa-Flood model and evaluated  
131 against the observed daily live reservoir storage.

132 We manually calibrated the H08 model by adjusting four parameters for each river basin, which include single-  
133 layer soil depth, gamma, bulk transfer coefficient, and tau (Hanasaki et al., 2008). We evaluated the model  
134 performance using the coefficient of determination ( $R^2$ ) and Nash-Sutcliffe Efficiency (NSE) for daily streamflow  
135 and reservoir live storage. In addition, we compared the simulated and satellite-based observed flood occurrences.  
136 The satellite-based flood occurrence is calculated using the Global Surface Water (GSW) dataset (Pekel et al.,  
137 2016), available for the 1984-2020 period. We forced the well-calibrated combined (H08 and CaMa-Flood)  
138 models with observed meteorological forcing from India Meteorological Department (IMD) at 0.25° spatial  
139 resolution to conduct simulations from 1901 to 2020. The H08 model simulated runoff is used in CaMa-Flood to  
140 rout flood dynamics at six arc-minutes (0.1 degrees). We generated the flood depth maps for the historical worst  
141 flood at the sub-basin level. The worst flood is based on the highest magnitude of river flow observed at the  
142 subbasin outlet. The generated flood depths at 6 arc-minutes (0.1°) were further downscaled to 1 arc-minute  
143 (~0.185 km) resolution using the downscaling module available within the CaMa-Flood.

144 We used C-ratio (Nilsson et al., 2005; Zajac et al., 2017) to assess the potential impact of dams along a river. The  
145 C-ratio is an identifier calculated as the ratio of total maximum storage capacity of the upstream reservoirs to the  
146 mean annual discharge at a gauge station in the downstream region (Nilsson et al., 2005; Zajac et al., 2017). We  
147 calculated the C-ratio at the outlets of each sub-basins that are influenced by the presence of dams. A C-ratio of  
148 less than 0.5 indicates that the sub-basin is minimally affected by the presence of dams. Further, to identify sub-

149 basins susceptible to flood inundation resulting from dam operations, we multiplied the percentage of flooded  
150 area in each sub-basin by its corresponding C-ratio. This enabled us to identify the sub-basins that experience  
151 substantial flood inundation and are considerably impacted by the presence of reservoirs. Finally, we estimated  
152 the exposed rail and road infrastructure affected by floods. The flooded area overlapped over the road and railway  
153 network to estimate the network length affected by floods in a sub-basin. We considered the flooded area of the  
154 observed worst flood. The subbasins with the highest rail and road infrastructure exposure to floods were  
155 identified.

## 156 **2.3 Risk assessment**

157 We estimated flood risk using hazard, exposure, and vulnerability based on the common framework adopted by  
158 the United Nations in the Global Assessment Reports of the United Nations Office for Disaster Risk Reduction  
159 (UNISDR, 2011, 2013). A similar framework was used in previous studies for flood risk assessments (C. M. R.  
160 Mateo et al., 2014; Tanoue, 2020; Winsemius et al., 2013). We multiplied the normalized values of hazard,  
161 exposure, and vulnerability to estimate the risk as:

$$162 \quad \textit{Risk} = \textit{Vulnerability} * \textit{Exposure} * \textit{Hazard} \quad \dots \dots (1)$$

163 The flood risk assessment can help identify the hotspots and prioritize climate adaptation (de Moel et al., 2015).  
164 Among the three components, vulnerability is a degree of damage to a particular object at flood risk with a  
165 specified amount and present on a scale from 0 to 1. We obtained the vulnerability index for each district from  
166 the “Climate Vulnerability Assessment for Adaptation Planning in India Using a Common Framework”, a report  
167 developed by the Department of Science and Technology  
168 (<https://dst.gov.in/sites/default/files/Full%20Report%20%281%29.pdf>). The vulnerability of each district is  
169 calculated using 14 indicators, each with equal weights. The indicators capture both sensitivity and adaptive  
170 capacity. We estimated the vulnerability index of each sub-basin by taking the spatial mean of the vulnerability  
171 of the districts falling into the sub-basins. Exposure is termed as assets and population in a flood-exposed area  
172 resulting in flood damage (Marchand et al., 2022). The population dataset is a critical component in performing  
173 exposure estimation. The exposure is defined as the fraction of the population exposed to the flood extent (Smith  
174 et al., 2019). We completed the flood exposure estimate using the Global Human Settlement Layers (GHSL)  
175 population dataset (Joint Research Centre (JRC) et al., 2021), which is available at a resolution of 30 arc-seconds  
176 for 1975, 1990, 2000, 2014 and 2015. We used the population data for the year 2015 throughout this study. We  
177 rescaled the population data to 6 arc-minutes to make it consistent with the flooded area simulated from the  
178 combined model. We estimated the hazard as the exceedance probability of a flooded area exceeding half of the  
179 historical maximum flooded area in the last 50 years. We used normalized vulnerability, exposure, and hazard to  
180 estimate the risk.

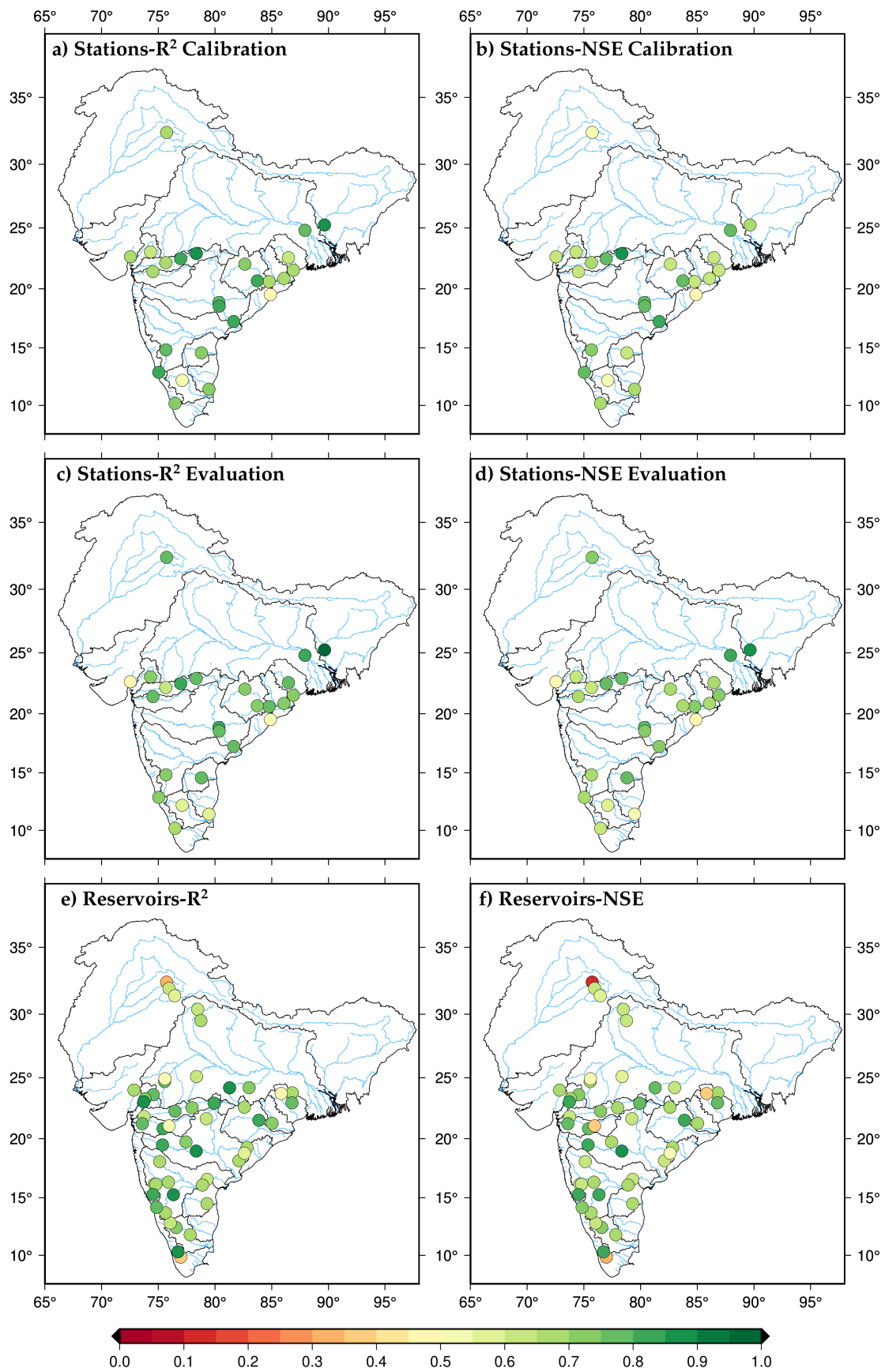
## 181 **3. Results**

### 182 **3.1 Calibration and evaluation of hydrological models**

183 We calibrated and evaluated the performance of the H08 and CaMa-Flood combined models against the observed  
184 daily streamflow (Figure 1). Due to the unavailability of daily observed streamflow for the three transboundary  
185 river basins (Indus, Ganga and Brahmaputra), we used observed monthly streamflow to calibrate the model. In

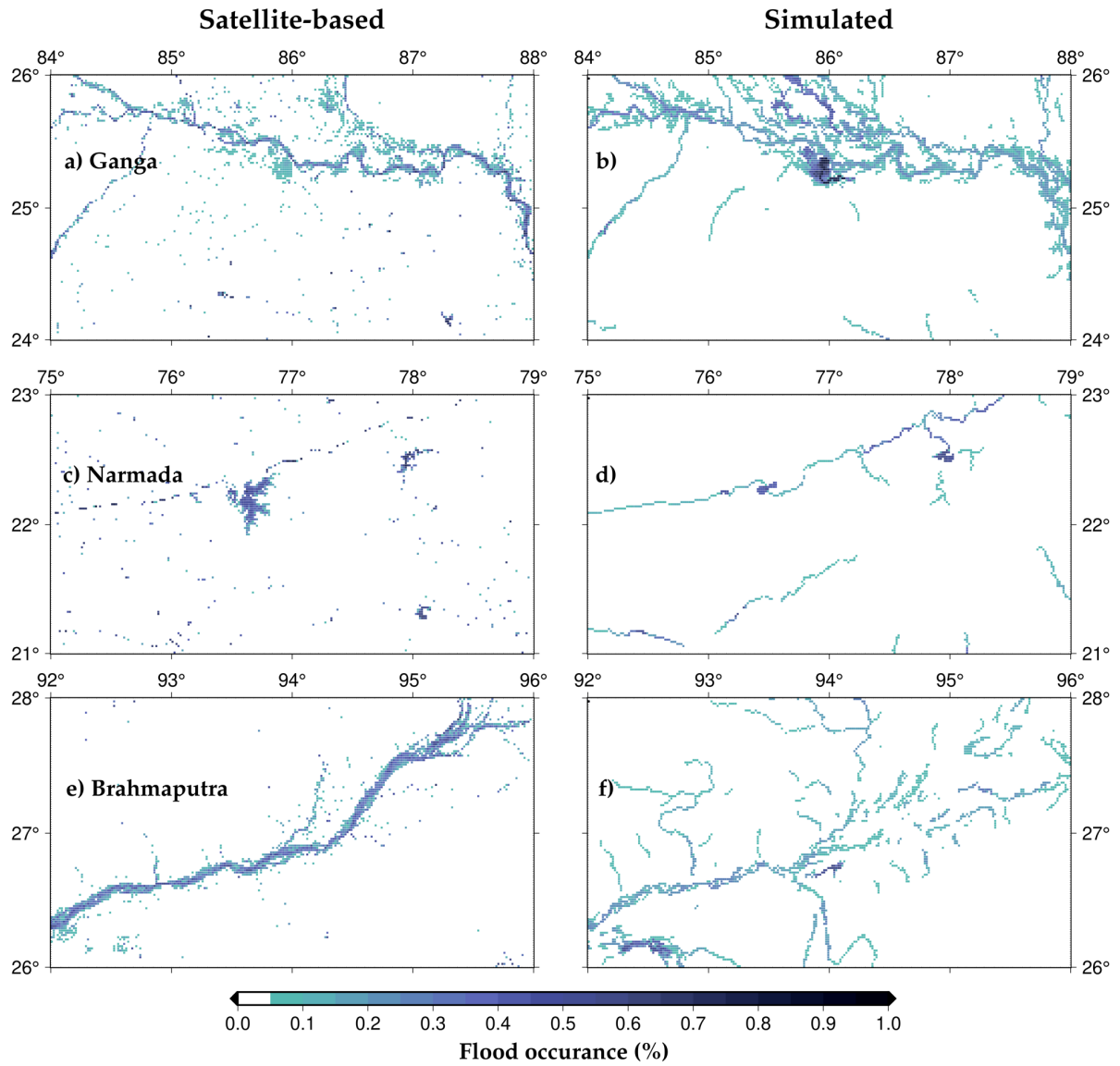
186 addition, we evaluated the model performance for daily live storage of the 51 reservoirs after the calibration  
187 against the observed flow (Figure 1). The model exhibited good skills ( $R^2 > 0.6$  and  $NSE > 0.6$ ) for almost all the  
188 river basins except Cauvery, East Coast, Northeast Coast, and Sabarmati. The model also performed well with  
189  $NSE$  greater than 0.6 for more than 80% of the selected reservoirs in simulating daily live storage for the selected  
190 reservoirs. We estimated the bias and timing error in simulating peak discharge at all the selected gauge stations  
191 (Figure S2). We calculated the bias in the model simulated annual maximum streamflow against the observed  
192 annual maximum streamflow for the time periods for which observations are available. We excluded the  
193 transboundary rivers (Ganga, Brahmaputra and Indus) as timing error (in days) could not be estimated due to the  
194 unavailability of daily observed flow. While other gauge stations exhibited moderate bias, gauge stations in  
195 Cauvery, Sabarmati, and Mahi rivers basins show a considerable dry bias. Contrary to several other stations where  
196 the mean timing error was below two days, the Sabarmati river basin displayed a comparatively higher mean  
197 timing error. The relatively poor performance of the model in these river basins can be attributed to the lack of  
198 long-term observations as well as substantial human interventions that can affect the observed flow.

199 We compared model-simulated, and satellite-based observed flood occurrence for the 1984-2020 period (Figure  
200 2). In addition, we compared the model-simulated flood events against Sentinel-1 SAR and MODIS satellite-  
201 based imagery for a few flood events based on the satellite data availability (Figures. 3, S3, S4). We found that  
202 the model simulated flood extent captures the satellite based flood extent. However, we note that the model  
203 overestimated the flood extent in Ganga river basin and underestimated in Brahmaputra river basin, therefore,  
204 showing a non-systematic bias. Moreover, a considerable difference in the flood extent based on the two satellite  
205 datasets was observed, which highlights the observational uncertainty in the estimation of flood extent. In general,  
206 the model exhibits satisfactory performance in simulating flood extent against the satellite-based observations.  
207 However, the model overestimates flood extent in the Ganga basin, which could be attributed to the influence of  
208 cloud contamination and dense vegetation cover on satellite-based flood estimates (Chaudhari & Pokhrel,  
209 2022). On the other hand, the model underestimates the flood occurrence in the upstream region of the  
210 Brahmaputra River. This could be due to limitations in model parameterization, as observed flow is limited in the  
211 transboundary river basins. Despite the good performance against the observed streamflow, the simulated flood  
212 extent has a considerable bias, which can be attributed to satellite-based flood extent mapping limitations and the  
213 model's ability to capture the flood extent accurately. The model-simulated flood extent shows a good agreement  
214 against the reported flood from EM-DAT and DFO databases (Figure S5). In addition, the simulated flood extent  
215 also showed a good agreement with the reported flood in cities in the Brahmaputra and Ganga River basins. Given  
216 the limitation in the streamflow and flood extent observations, the hydrological models perform satisfactorily and  
217 can be used for the sub-basin level risk assessment.



218

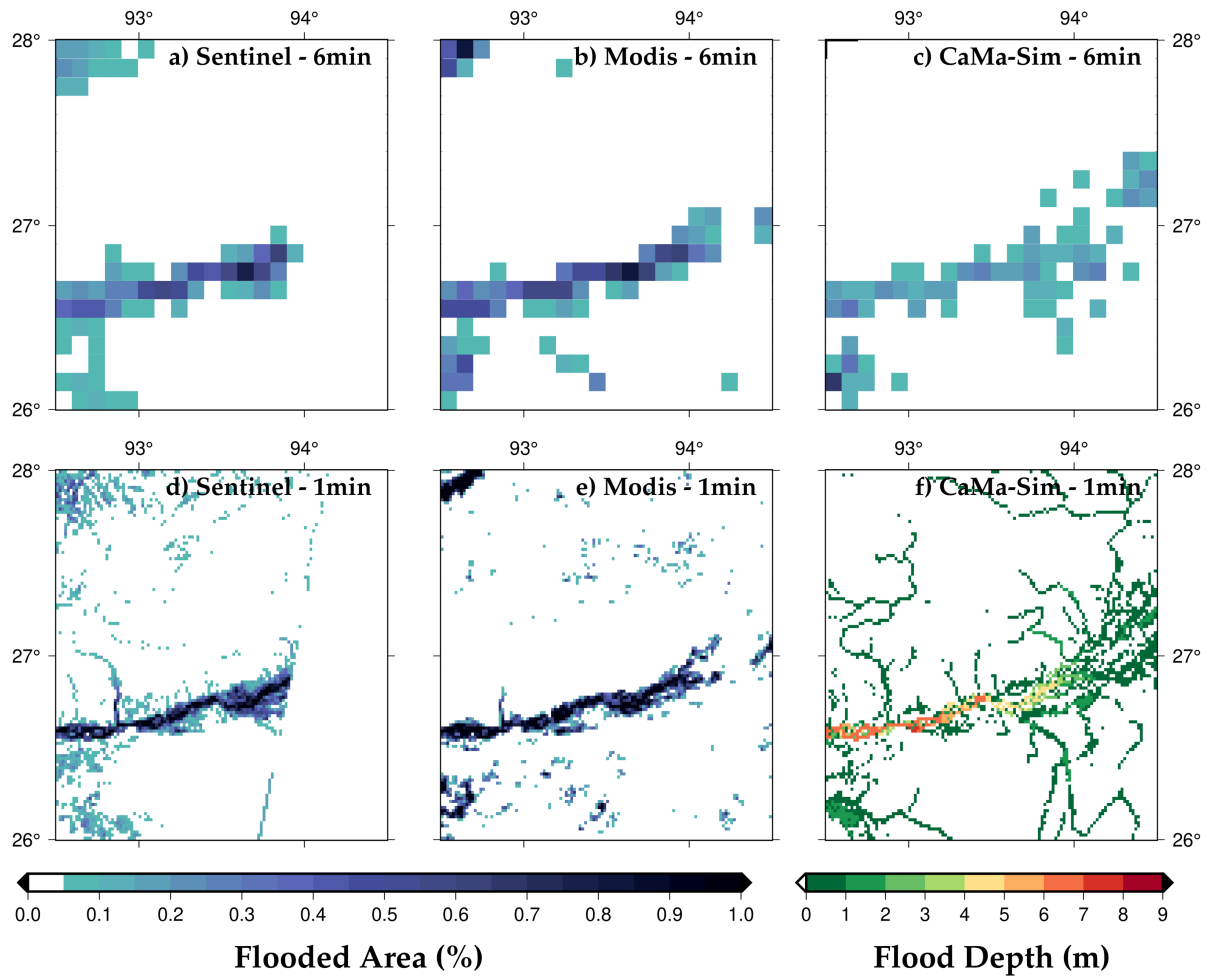
219 **Figure 1: Calibration and evaluation of the combined model for daily river flow and reservoir storage at**  
 220 **gauge stations and daily live storage of reservoirs**



221

222 **Figure 2: Simulated flood occurrences compared with satellite-based flood occurrence for different**  
 223 **regions in Ganga, Narmada and Brahmaputra River basin.**





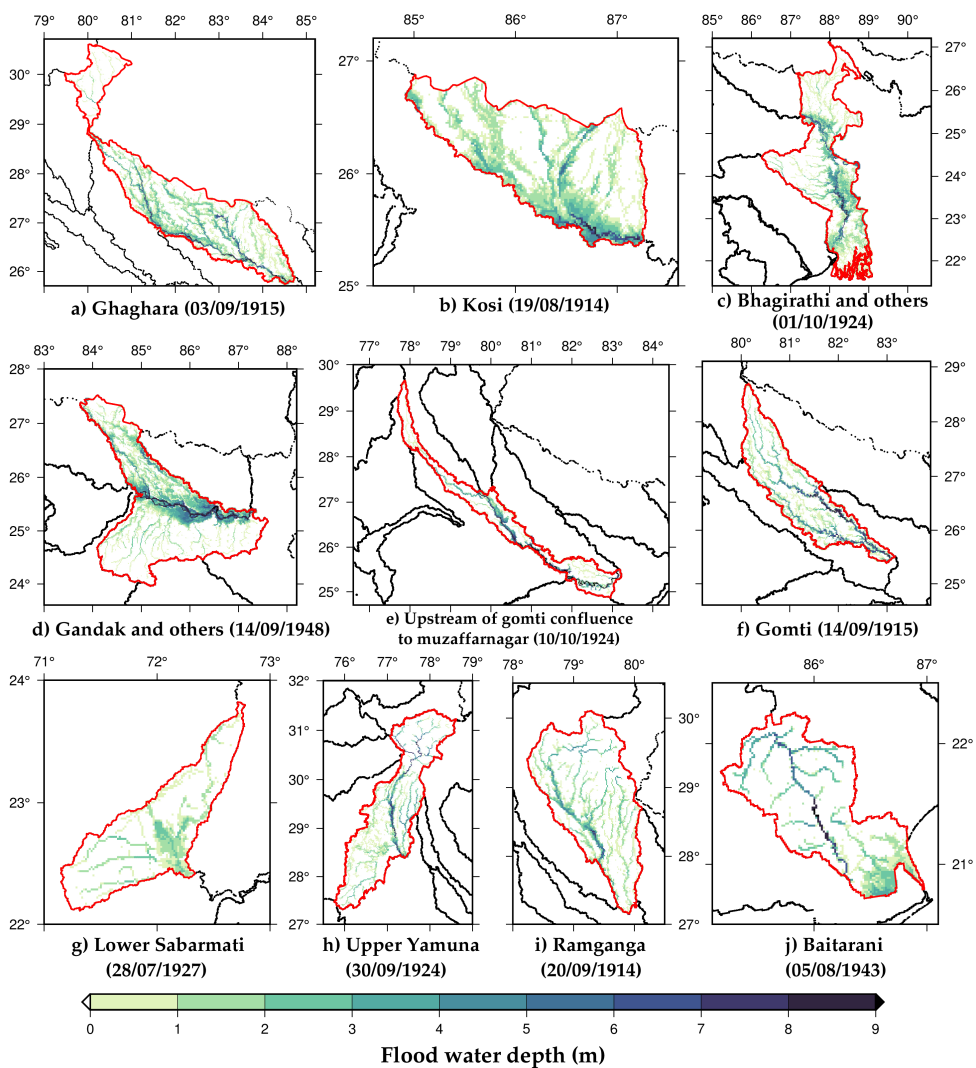
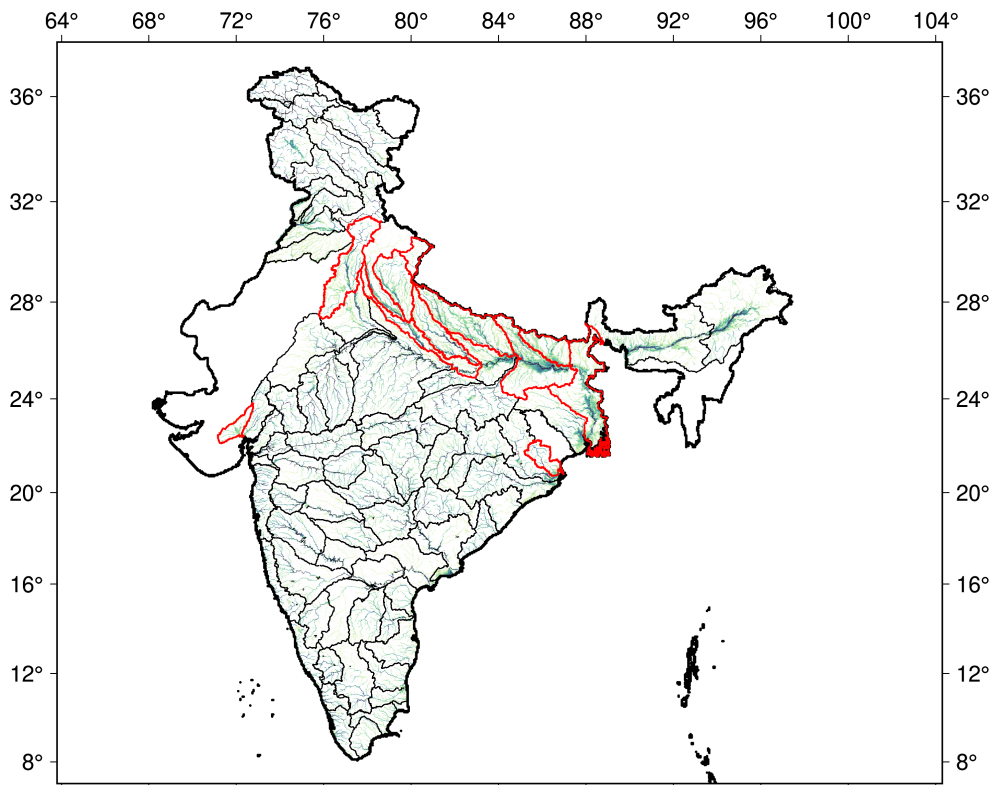
224

225 **Figure 3: Simulated flood extent compared with Sentinel-1 SAR and MODIS satellite-based flood extent**  
 226 **for the 2016 flood event in the Brahmaputra river**

227 **3.2 Estimation of the observed flood extent**

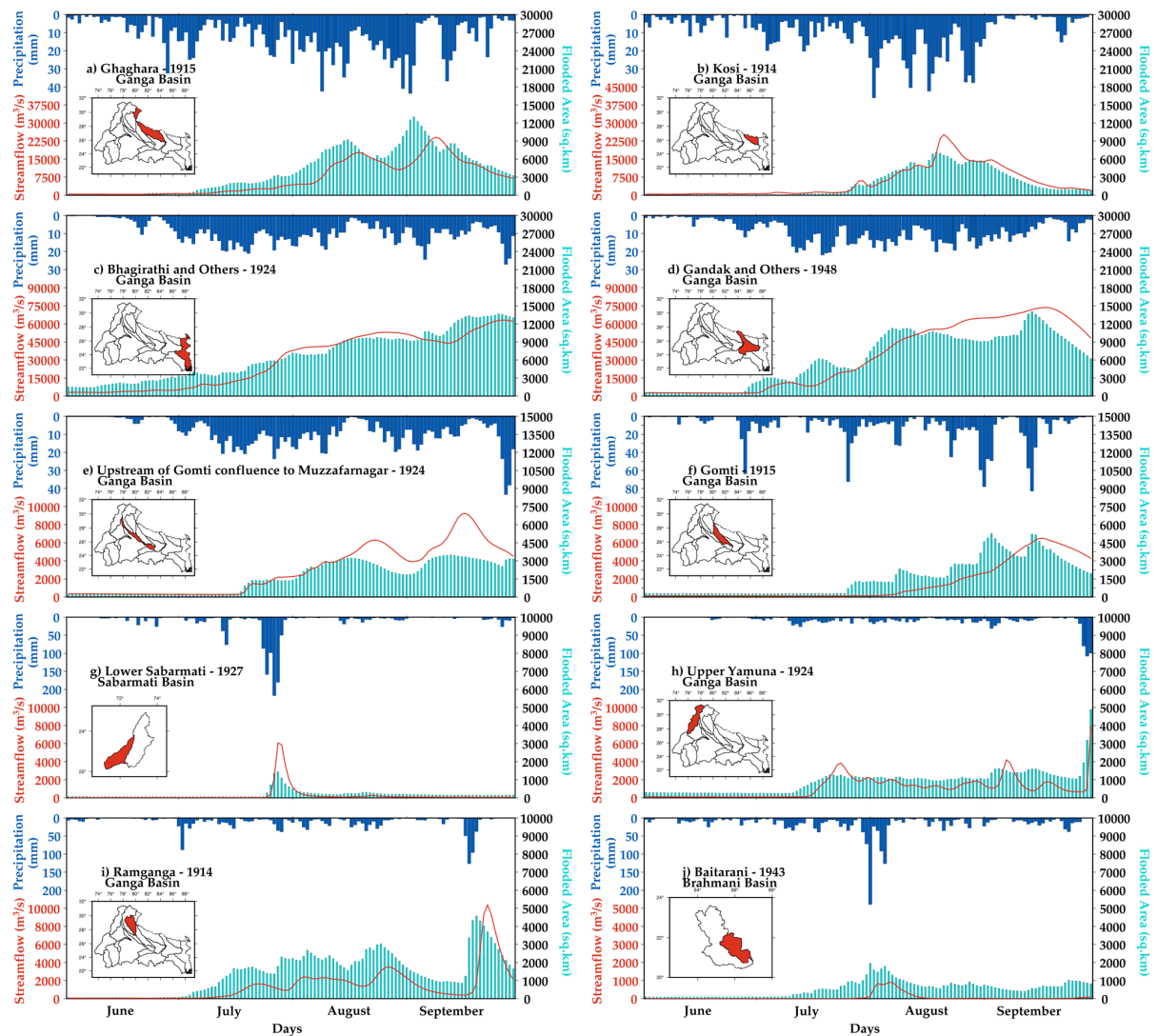
228 Next, we reconstructed the flood inundation for the observed worst flood for each sub-basin for the 1901-2020  
 229 period in India. The inundation extent for the worst flood can help us identify the sub-basin with higher flood risk.  
 230 We estimated flood depth and inundated area for each sub-basin for the worst flood during the last 120 years  
 231 (Figure 4). In addition, we identified the occurrence of the worst flood at the sub-basin level during the 1901-2020  
 232 period. We highlighted ten sub-basins that experienced the highest fractional area affected by the worst flood.  
 233 Sub-basins in the Ganga and Brahmaputra rivers are among the most highly influenced by the worst flood. For  
 234 instance, Ghaghra, Kosi, Bhagirathi, Gandak, Gomti, lower Sabarmati, upper Yamuna, Ramganga, and Baitarani  
 235 sub-basins had the highest fractional area affected by the worst flood during 1901-2020 (Figure 4). The fractional  
 236 area of sub-basins in the semi-arid western India is less affected compared to those located in the Ganga basin.  
 237 For example, the lower Sabarmati sub-basin of the Sabarmati River basin is among the sub-basins that are highly  
 238 influenced by the observed worst flood. We also find that the worst flood in the same year did not affect all the  
 239 sub-basins within a river basin (Figure S6). For instance, all the highly influenced sub-basins experienced the  
 240 worst flood in different years in the Ganga basin (Figure 4). Most of the top flood-affected sub-basins experienced  
 241 floods during August-September in the summer monsoon season. Overall, the flood extent due to the worst flood

242 is substantially greater in the sub-basins of the Ganga and Brahmaputra river basins compared to other basins in  
243 India (Figure 4). Ganga river basin also has the highest population density among all the basins in the Indian sub-  
244 continent, which makes it vulnerable for the flood risk.



246 **Figure 4: Flood depth map for the observed worst flood for each sub-basins, highlighting the sub-basins**  
247 **with maximum flood inundated area (%) (a) Ghaghara – Ganga River basin (b) Kosi – Ganga River basin**  
248 **(c) Bhagirathi and others – Ganga River basin (d) Gandak and others – Ganga River basin (e) Upstream**  
249 **of Gomti confluence to Muzaffarnagar – Ganga River basin (f) Gomti – Ganga River basin (g) Lower**  
250 **Sabarmati – Sabarmati River basin (h) Upper Yamuna – Ganga River basin (i) Ramganga – Ganga River**  
251 **basin (j) Baitarani – Brahmani River basin**

252 Next, we examined the precipitation, streamflow, and flood-affected area (%) for the ten sub-basins that had the  
253 highest fractional flood affected area for the worst flood during 1901-2020 (Figure 5). As floods mostly occur  
254 during the summer monsoon season in India (V. Mishra et al., 2022; Nanditha & Mishra, 2021), we examined  
255 the temporal variability of precipitation, and streamflow during the monsoon season of the worst flood year.  
256 Nanditha and Mishra (2022) reported that multi-day precipitation is India's most robust driver of floods. Moreover,  
257 extreme precipitation and wet-antecedent conditions trigger floods in India (Nanditha & Mishra, 2022). We  
258 find that the Ghaghara sub-basin of the Ganga river experienced the worst flood in September 1915, affecting  
259 more than 10,000 km<sup>2</sup> area of the sub-basin. A multi-day rainfall in late August and early September (1915) caused  
260 the worst flood in the basin. The Kosi sub-basin of the Ganga river experienced the worst flood in August 1914,  
261 which affected more than 5000 km<sup>2</sup> of the basin (Figure 5). Similarly, Bhagirathi and other sub-basins in the  
262 Ganga river basin were affected by the worst flood in late September 1924, which inundated more than 12000  
263 km<sup>2</sup> of the sub-basin. Similarly, Gandak and Gomti river basins experienced the worst floods in 1948 and 1915,  
264 respectively. Our results agree with the information presented in previous studies (Agarwal & Narain, 1991;  
265 Fredrick, 2017; Joshi, 2014; D. K. Mishra, 2015; A. Singh et al., 2021). We find that most of the sub-basins  
266 of the Ganga river basin are prone to large extents of flood inundation. Moreover, the worst floods in most sub-  
267 basins were caused by multi-day precipitation, a prominent driver of floods in the Indian sub-continental river  
268 basins (Figure 5).

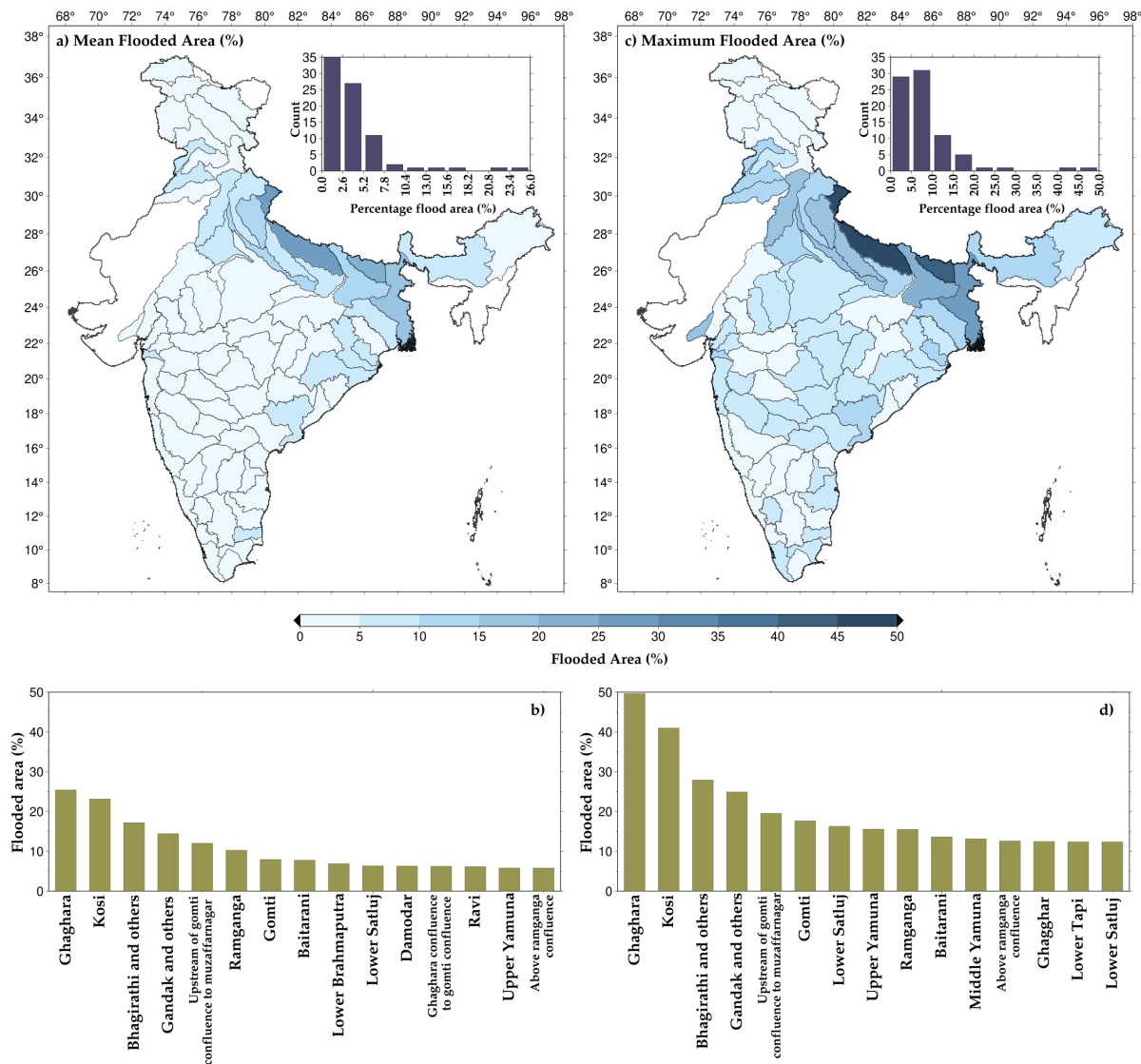


269

270 **Figure 5: Daily upstream precipitation (mm, blue), the H08 model simulated streamflow (red) at the sub-**  
 271 **basin outlet (m<sup>3</sup>/s), and flooded area (km<sup>2</sup>, green) for the summer monsoon (June-September) period of**  
 272 **the corresponding worst flood year. (a) Ghaghara - Ganga River basin (b) Kosi - Ganga River basin (c)**  
 273 **Bhagirathi and others - Ganga River basin (d) Gandak and others - Ganga River basin (e) Upstream of**  
 274 **Gomti confluence to Muzaffarnagar - Ganga River basin (f) Gomti - Ganga River basin (g) Lower**  
 275 **Sabarmati – Sabarmati River basin (h) Upper Yamuna – Ganga River basin (i) Ramganga – Ganga River**  
 276 **basin (j) Baitarani – Brahmani River basin**

277 To further examine the flood-affected area at the sub-basin level, we estimated the mean annual maximum flooded  
 278 area (Figure 6a) and historical maximum flooded area using the H08-CaMa flood models (Figure 6b). Most of the  
 279 highly flooded sub-basins are in the Ganga River basin. While the mean annual maximum flooded area for the  
 280 top flood-affected sub-basins ranged between 10 to 15%, their maximum flooded area varied between 30 to 40%.  
 281 Other than sub-basins from the Ganga river basin, Baitarani, lower Tapi, lower Godavari, Brahmani, and lower  
 282 Mahanadi also showed a considerable mean flooded area during the 1901-1920 period. In the case of the maximum  
 283 flooded area, Gandak, Kosi, and Ghaghara confluence to Gomti confluence sub-basins exhibited more than 20%  
 284 flooded area. Sub-basins from the other river basins, such as lower Tapi, lower Narmada, Baitarani, and lower

285 Satluj, are in the top fifteen sub-basins with the highest flooded area. The sub-basins in the Ganga and  
 286 Brahmaputra rivers are the most flood-affected. Moreover, the Ganga and Brahmaputra rivers experience the  
 287 highest floods among all the river basins (Mohanty et al., 2020; Mohapatra & Singh, 2003).



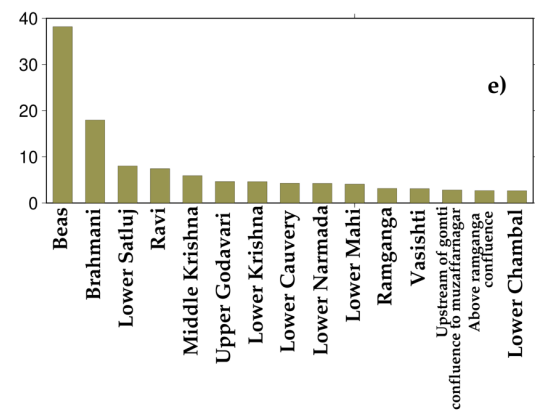
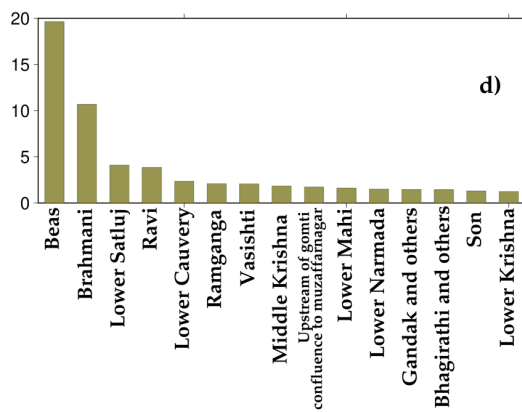
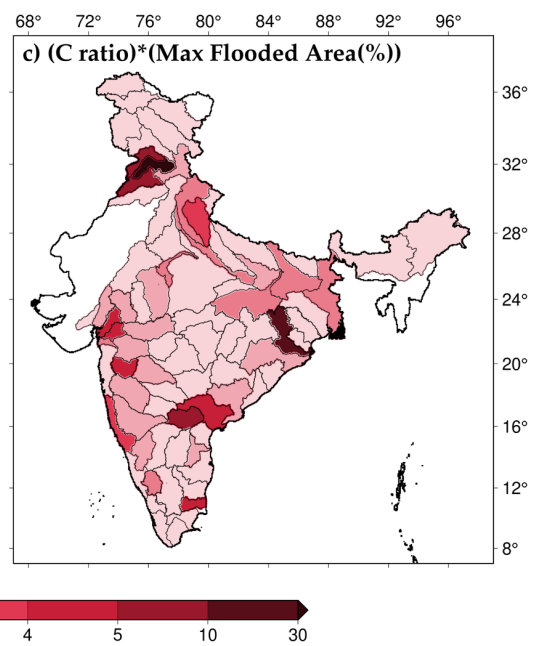
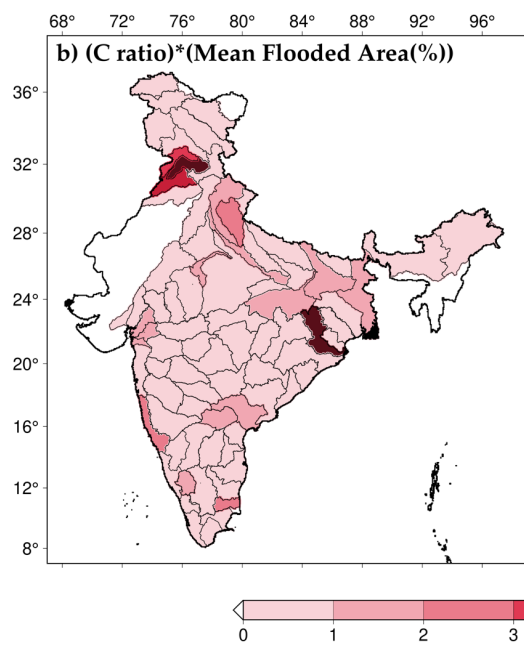
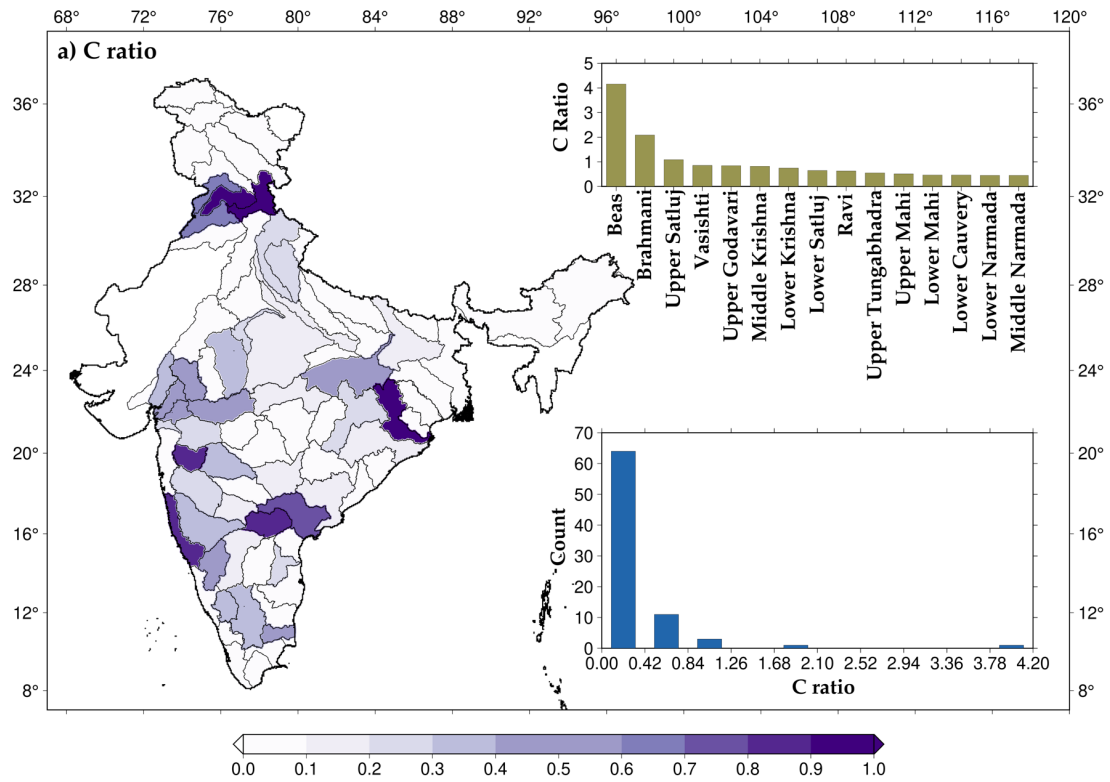
288

289 **Figure 6: (a) Mean of annual maximum flooded area (percentage) between 1901-2020 and the overall**  
 290 **distribution (b) highlighting the top fifteen sub-basin. (c) Historical maximum flooded area (percentage)**  
 291 **and the overall distribution (d) highlighting the top fifteen sub-basin.**

### 292 3.3 Influence of reservoirs on flood extent

293 We selected and considered 51 major reservoirs to examine their influence on flood risk based on the availability  
 294 of the observed storage data. We estimated C-ratio for each sub-basin considering the river flow at the outlet to  
 295 investigate the impact of reservoirs on streamflow. C-ratio can vary between zero to infinity, and higher values  
 296 indicate the prominent effect of dams on river flow. We identified sub-basins with a greater influence on dams  
 297 based on the C-ratio. We find that Beas, Brahmani, upper Satluj, Upper Godavari, Middle and Lower Krishna,  
 298 and Vashishti are among the most influenced by the dams. Beas sub-basin has the highest C-ratio (4.16) among

299 all the sub-basin in the Indian sub-continent (Figure 7a). Out of the 80 sub-basins, only eleven have C-ratio greater  
300 than 0.5. 64 out of 80 sub-basins have a C-ratio between zero to 0.42 (Figure 7a). We considered only 51 major  
301 reservoirs in our analysis. However, there are several major and minor dams for which observed data is  
302 unavailable. Therefore, the influence of reservoirs based on the C-ratio might need to be considered. However,  
303 our analysis indicates that dams in a few sub-basins can significantly alter the river flow and flood risk. For  
304 instance, dams effectively alter extreme flow's timing, duration, and frequency (Mittal et al., 2016). C-ratio alone  
305 may not effectively capture the influence of dams on floods; therefore, we multiplied the fractional area affected  
306 by floods and the C-ratio for each sub-basins. For instance, if a sub-basin is considerably affected by dams and  
307 has a large flood extent, the value of the multiplied ratio will be higher. The multiplier ratio can effectively identify  
308 the sub-basins with high flood-affected areas and flow regulated by the reservoirs. We find that Beas, Brahmani,  
309 Ravi, and Lower Satluj are among the highly influenced by floods and the presence of reservoirs. Overall, the  
310 sub-basins with higher C ratio and the highest flood-affected area are across the Indian subcontinent. Central India  
311 has sub-basins that are relatively less affected by floods and the presence of dams.

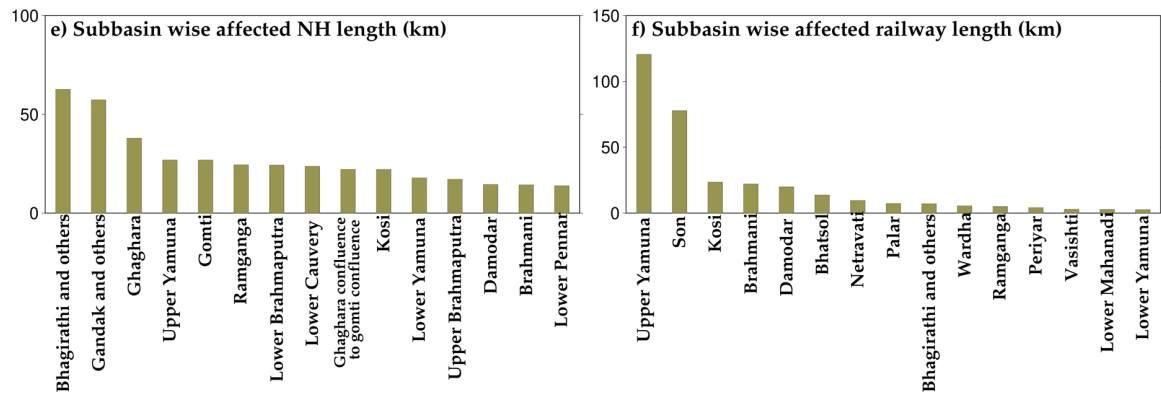
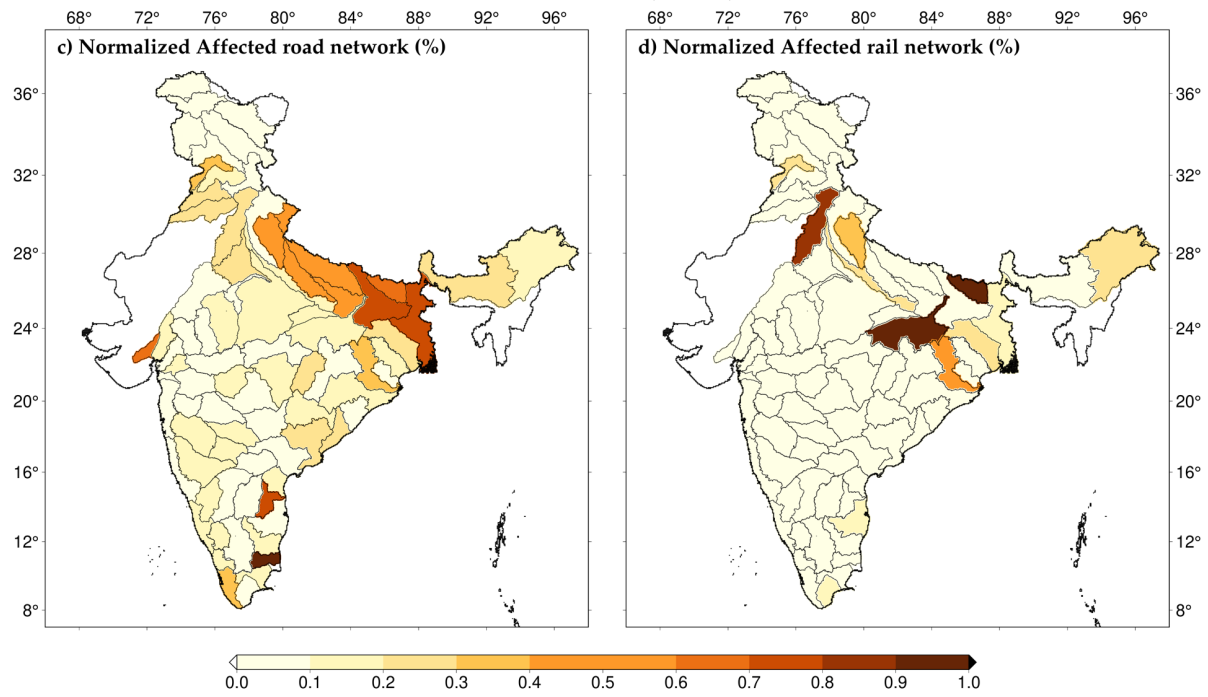
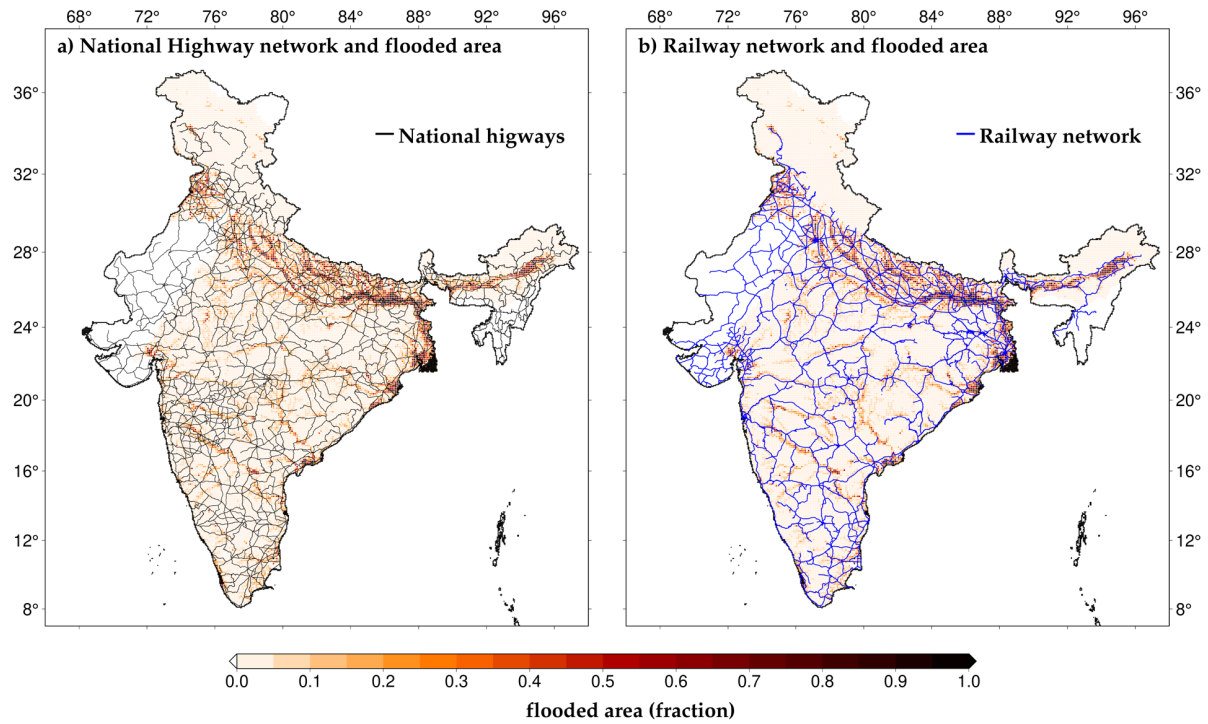




313 **Figure 7: (a) Sub-basin wise C-ratio, top fifteen sub-basins and distribution of sub-basins based on C-ratio**  
314 **values (b) Mean of annual maximum flooded area (percentage) multiplied with C-ratio (d) highlighting top**  
315 **15 sub-basins (c) Historical maximum flooded area (percentage) multiplied with C-ratio (e) highlighting**  
316 **top 15 sub-basins.**

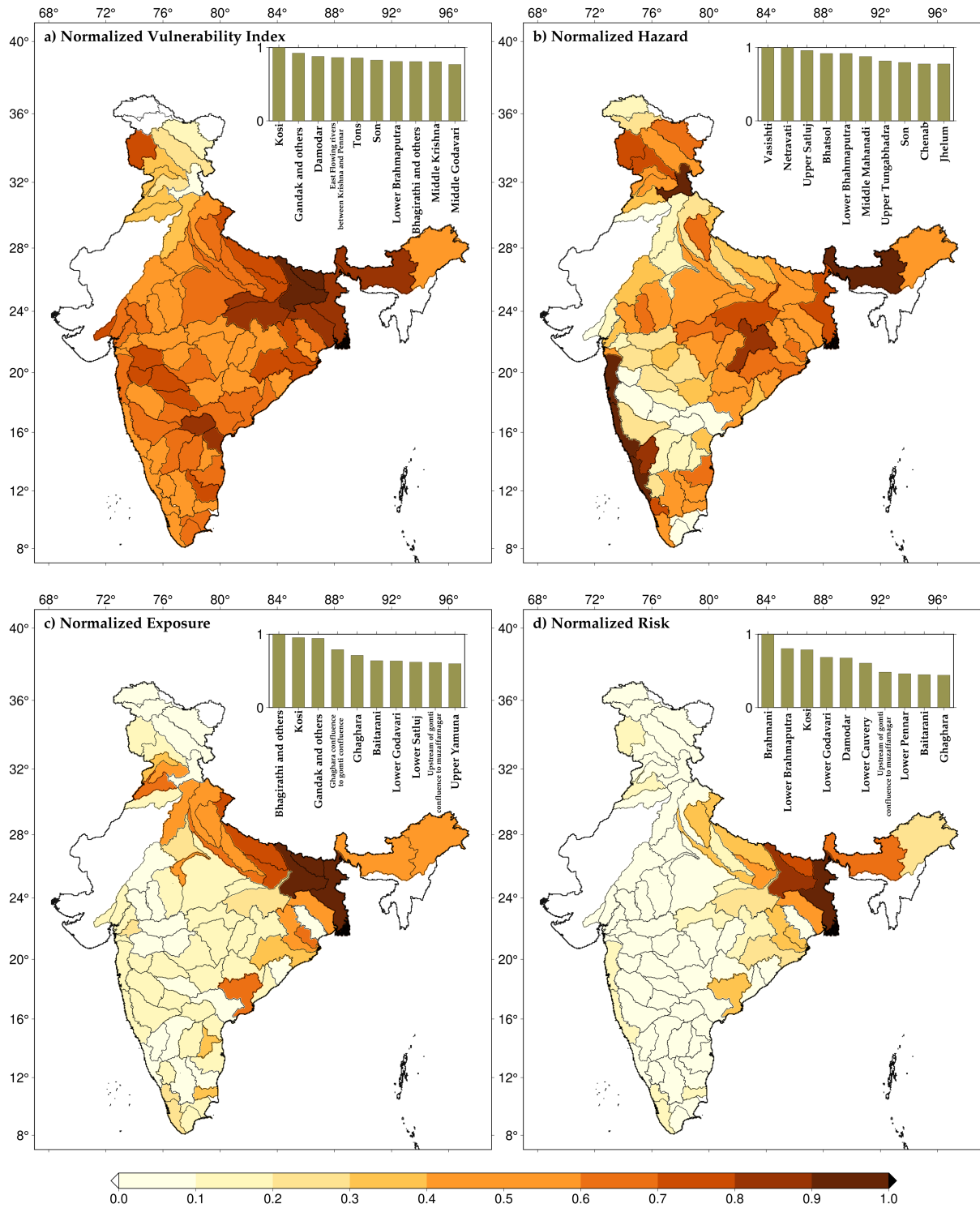
### 317 **3.4 Sub-basin level flood risk assessment**

318 Next, we identified the roads (national highways) and railway exposure to riverine floods for each subbasin.  
319 Climate change will adversely affect rail and road networks (Hooper & Chapman, 2012; Padhra, 2022). A  
320 considerable length of roads is affected due to surface flooding resulting from high-intensity rain (Koks et al.,  
321 2019). Therefore, we examined the impact of floods on rail and road infrastructure in India. We estimated the  
322 length of the road and railway network potentially affected by the worst flood that occurred during 1901-2020.  
323 We overlapped the road and rail network over the flooded area and estimated the network length exposed to floods  
324 (Figures 8a-b). The estimated length for each sub-basin was normalized between zero and one (Figures 8c-d). We  
325 find that the road network can be the most affected by the floods in the Gandak, Kosi and Ghaghara confluence  
326 to Gomti confluence in the Ganga river basin. On the other hand, a considerable part of the rail network can be  
327 affected by floods in Son, Kosi, and Upper Yamuna subbasins. Moreover, in Bhagirathi and Gandak river basins,  
328 more than 50 km of road network falls in the flood-prone regions (Figure 8e). There are ten sub-basins in which  
329 more than 20 km of road network falls in flood-prone areas of India. Similarly, over 20 km of the rail network is  
330 in the flood-affected areas of the six sub-basins (Upper Yamuna, Son, Kosi, Brahmani) [Figure 8f].



332 **Figure 8: Flood impacts on roads and railways infrastructure. (a-b) National Highways network and**  
333 **Railway network overlapped over the flooded area in worst flood cases, (c-d) subbasin wise normalised**  
334 **flood affected road and railway network (percentage), (e-f) top 15 subbasins with most affected national**  
335 **highways and railway length (km).**

336 Finally, we estimated sub-basin level flood risk using normalized vulnerability, hazard, and exposure (Figure 9).  
337 Vulnerability for each sub-basin in India was assessed using the national vulnerability assessment data available  
338 at the district level. We estimated hazard probability considering 50% of the inundated area for the worst flood as  
339 a benchmark. The likelihood of flood inundated areas in a sub-basin exceeding the benchmark was used in the  
340 risk assessment. Similarly, we used the worst flood extent and gridded population data to estimate flood exposure.  
341 The sub-basins in north-central India have a relatively higher vulnerability calculated using the socio-economic  
342 indicators. The vulnerability is relatively lower in north India and the Western Ghats. Kosi, Gandak, and Damodar  
343 sub-basins have the highest vulnerability. We find that hazard probability is higher in the sub-basins of  
344 Brahmaputra, rivers in the western Ghats, and a few sub-basins of the Indus river basin (Figure 9b). For instance,  
345 upper Satluj, Chenab, and Jhelum sub-basins of the Indus river have higher hazard probability. Other than the  
346 Western Ghats, most sub-basins in Peninsular India have relatively lesser hazard probability. Exposure, which  
347 represents the fraction of the population affected by flood under the worst flood scenario, is higher in the Indo-  
348 Gangetic Plain. Apart from the sub-basins of the Ganga River basin, the lower Brahmaputra, lower Godavari, and  
349 Baitarani sub-basin show higher exposure. Therefore, Ganga and Brahmaputra Rivers basins are the highest flood-  
350 prone river basins and have high flood exposure. Rentschler et al. (2022) also reported that the highest population  
351 exposure due to floods is in Uttar Pradesh, Bihar, and West Bengal, which is part of the Ganga river basin.



352

353 **Figure 9: Sub-basin level (a) Normalized vulnerability index (b) Normalized hazard (c) Normalized**  
 354 **exposure (d) Normalized risk. The top 10 sub-basins are highlighted as bars in panels inside the figures.**

355 We estimated the flood risk for each sub-basin, a collective representation of vulnerability, hazard, and exposure.  
 356 As expected, the flood risk is higher in the Ganga and Brahmaputra river basins compared to other parts of the  
 357 country. The higher flood risk in these basins can be attributed to higher vulnerability, hazard probability, and  
 358 exposure. For instance, Bhagirathi, Gandak, Kosi, lower Brahmaputra, and Ghaghara are the sub-basins with the  
 359 highest flood risk in India (Figure 9d). Despite the higher hazard probability in the sub-basins of the Indus and

360 west coast river basins, the overall flood-risk is considerably lower than the sub-basins of the Ganga and  
361 Brahmaputra river basins primarily due to less vulnerability and exposure. Our results show that flood risk in  
362 some of the sub-basins of the Ganga and Brahmaputra river basins can be reduced by reducing the vulnerability.

#### 363 **4. Discussion and conclusions**

364 Flood risk mapping is essential for risk reduction and developing mitigation measures. The flood risk will likely  
365 increase due to increased hazard probability and exposure (Ali et al., 2019). Hirabayashi et al. (2013) showed that  
366 a warmer climate would increase the risk of floods on a global scale. In India also, floods are expected to become  
367 more likely under warming climate. For instance, Ali et al. (2019) reported that multi-day floods are projected to  
368 rise faster than single-day flood events. The projected rise in the flood frequency in India can be attributed to  
369 increased extreme precipitation under warming climate (Mukherjee et al., 2018). Observational studies have also  
370 concluded that there has been a considerable rise in extreme precipitation in India during the summer monsoon  
371 season (Roxy et al., 2017), which is linked to warming climate. While the warming climate is directly linked to  
372 the increased frequency of extreme precipitation, its association with riverine floods is not straightforward. For  
373 instance, Nanditha & Mishra (2021, 2022) reported that multi-day precipitation on the wet antecedent condition  
374 is the most favourable conditions for riverine floods in India.

375 While mapping the flood risk at appropriate spatial resolution is complex and challenging, it is vital for disaster  
376 risk reduction. Flood inundation mapping that provides the spatial extent of flooding is crucial as the first  
377 responders use it during a flood emergency (Apel et al., 2009). There are several approaches to mapping flood  
378 inundation (Teng et al., 2017). We used hydrodynamic modelling to develop long-term flood inundation maps for  
379 the Indian sub-basins. Creating high-resolution flood inundation maps based on hydrodynamic modelling is  
380 computationally expensive (Dottori et al., 2016) for a large domain like India. In addition, higher-resolution flood  
381 risk mapping that can be used at the local scale for decision-making requires accurate terrain information and river  
382 cross-section datasets that are not available. For instance, freely available digital elevation models (DEM) can be  
383 too coarse to resolve the flood inundation and depth variability at a local scale (Cook & Merwade, 2009; Dey  
384 et al., 2022). The uncertainties within hydrologic outputs can primarily arise due to inaccuracies in both input  
385 data and model parameterization (Poulin et al., 2011). Inaccuracies in input meteorological data may stem from  
386 disparate sources, leading to errors in spatial and temporal interpolation (Brown & Heuvelink, 2005). Similarly,  
387 model parameterization errors, which involve assigning values to parameters governing diverse hydrological  
388 processes, can emerge during the calibration process (Laiolo et al., 2015). Moreover, there are uncertainties  
389 originating from utilizing long-term flood occurrence data to assess flood mapping capabilities. Our modelling  
390 framework that considers the influence of reservoirs provides sub-basin scale flood inundation extent as our aim  
391 was to provide a long-term assessment of flood extent in at the country scale. Additionally, downscaling of flood  
392 depths introduces biases as coarse-scale information is translated to the local scale (He et al., 2021), which might  
393 have considerable deviations from the actual observed flood extent. Given these limitations, our findings provide  
394 valuable information based on the long-term record developed using model simulations that can be used for the  
395 regional scale policy development for flood mitigation. Cloud cover during the summer monsoon, when most  
396 floods occur in India (Nanditha et al., 2022), hinders the utility of satellite data for flood inundation mapping. We  
397 calibrated and evaluated our H08-CaMa flood modelling framework using the observed flow, reservoir storage,

398 and satellite-based inundation. However, all these datasets available from the in-situ network or satellites are  
399 prone to errors and uncertainty (Di Baldassarre & Montanari, 2009; Stephens et al., 2012; Teng et al.,  
400 2017). We used C-ratio as an indicator to quantify the influence of dams on streamflow. However, C-ratio may  
401 not fully capture the complexities and variations in the impacts of reservoir operations. Furthermore, in case of  
402 run-of-the-river (RoR) dams, the C-ratio may over-estimate the downstream hydrological impacts. Therefore, C-  
403 ratio may not solely capture the downstream hydrological effects resulting from dams. Nevertheless, it provides  
404 preliminary information on the potential dam influence on the downstream flow.

405 India has implemented several flood risk mitigation measures at multiple government levels. The construction of  
406 embankments along rivers is a common flood risk mitigation measure in India. These embankments help contain  
407 the floodwaters within the river channels and protect nearby areas from inundation (NDMA, 2016). The CWC in  
408 India operates a network of flood forecasting stations that collect real-time data on rainfall and water levels to  
409 forecast floods and issue warnings to vulnerable communities. Notwithstanding the considerable investments and  
410 flood-control measures, India has witnessed substantial mortality, human migration, and economic loss. Flood  
411 mortality has increased mainly because of increased frequency, not necessarily due to increased flood intensity  
412 (Hu et al., 2018). About 3% of the total geographical area of India is affected by floods every year that cause  
413 damage to agriculture and infrastructure. The top ten floods that occurred during 1985-2015 caused the mortality  
414 of more than 1000 people while more than 35 million people were displaced due to floods between 2000-2004  
415 (Dartmouth Flood Observatory). The recent riverine floods in Uttarakhand and Kerala highlighted the growing  
416 flood risk in India, which warrants the need for flood mitigation. The recent flood in August 2022 in Pakistan  
417 caused an estimated loss of \$30 billion. Both structural and non-structural measures are required for flood  
418 mitigation (Nanditha & Mishra, 2021). Our risk assessment provides policy implications towards reducing  
419 vulnerability to reduce the flood risk. Moreover, a sub-basin level ensemble forecast is needed to be used for early  
420 flood warnings in the sub-basins with higher flood risk.

421 Based on our findings, the following conclusions can be made:

- 422 • The coupled hydrological and hydrodynamic modelling framework based on the H08-CaMa Flood model  
423 was used to estimate the flood risk assessment in India. The hydrological modelling framework  
424 performed well against the observed flow, reservoir storage, and satellite-based flood inundation. The  
425 role of 51 major reservoirs was considered in flood risk assessment based on the long-term simulations  
426 for the 1901-2020 period.
- 427 • The sub-basins in the Ganga and Brahmaputra river basins experienced the most significant flood extent  
428 during the worst flood in 1901-2020. Similarly, the mean annual maximum flood extent is higher for the  
429 sub-basins in the two major transboundary river basins (e.g., Ganga and Brahmaputra). The worst flood  
430 affected different sub-basins on the two main flood-affected river basins in different years. Major floods  
431 in the flood-prone sub-basins of the Ganga and Brahmaputra basins occur during the summer monsoon  
432 season, especially during the August-September period.
- 433 • The sub-basins with a more prominent influence of dams based on the C-ratio were identified. Beas,  
434 Brahmani, upper Satluj, Upper Godavari, Middle and Lower Krishna, and Vashishti sub-basins are

435 among the most influenced by the dams. Moreover, Beas, Brahmani, Ravi, and Lower Satluj are among  
436 the most affected by floods and the presence of reservoirs.

- 437 • Flood risk is higher in the Ganga and Brahmaputra river basins compared to other parts of the country.  
438 The higher flood risk in the two transboundary river basins can be attributed to higher vulnerability,  
439 hazard probability, and exposure. Bhagirathi, Gandak, Kosi, lower Brahmaputra, and Ghaghra are India's  
440 sub-basins with the highest flood risk.

441 **Data availability:** All the datasets used in this study can be obtained from the corresponding author.

442 **Competing interest:** Authors declare no competing interest.

443 **Author contributions:** VM designed the study. UV conducted the analysis and wrote the first draft. All the  
444 authors contributed in the writing and discussion.

445 **Acknowledgement:** The work was supported by the Monsoon Mission, Ministry of Earth Sciences. The authors  
446 acknowledge the data availability from India Meteorological Department (IMD) and India-WRIS. We  
447 acknowledge the database availability from EM-DAT: <http://www.emdat.be/>, DFO:  
448 <http://floodobservatory.colorado.edu>, population data from GHSL:  
449 <https://sedac.ciesin.columbia.edu/data/set/ghsl-population-built-up-estimates-degree-urban-smod>,  
450 vulnerability assessment data from DST: HYPERLINK  
451 "https://dst.gov.in/sites/default/files/Full%20Report%20%281%29.pdf" <https://dst.gov.in/sites/default/files/Full%20Report%20%281%29>  
452 <https://dst.gov.in/sites/default/files/Full%20Report%20%281%29>

## 453 References

454 Acreman, M. (2000). *Managed Flood Releases from Reservoirs: Issues and Guidance*.  
455 [https://sswm.info/sites/default/files/reference\\_attachments/ACREMAN%202000%20Mana](https://sswm.info/sites/default/files/reference_attachments/ACREMAN%202000%20Managed%20Flood%20Releases%20from%20Reservoirs.pdf)  
456 [ged%20Flood%20Releases%20from%20Reservoirs.pdf](https://sswm.info/sites/default/files/reference_attachments/ACREMAN%202000%20Managed%20Flood%20Releases%20from%20Reservoirs.pdf)

457 Agarwal, A., & Narain, S. (1991). *Floods, flood plains and environmental myths*.

458 Ali, H., Modi, P., & Mishra, V. (2019). Increased flood risk in Indian sub-continent under the  
459 warming climate. *Weather and Climate Extremes*, 25, 100212.  
460 <https://doi.org/10.1016/J.WACE.2019.100212>

461 Allen, S. K., Linsbauer, A., Randhawa, S. S., Huggel, C., Rana, P., & Kumari, A. (2016).  
462 Glacial lake outburst flood risk in Himachal Pradesh, India: an integrative and anticipatory  
463 approach considering current and future threats. *Natural Hazards*, 84(3), 1741–1763.  
464 <https://doi.org/10.1007/s11069-016-2511-x>

465 Apel, H., Aronica, G. T., Kreibich, H., & Thielen, A. H. (2009). Flood risk analyses - How  
466 detailed do we need to be? *Natural Hazards*, 49(1), 79–98. [https://doi.org/10.1007/S11069-](https://doi.org/10.1007/S11069-008-9277-8/TABLES/5)  
467 [008-9277-8/TABLES/5](https://doi.org/10.1007/S11069-008-9277-8/TABLES/5)

468 Bernhofen, M. V., Cooper, S., Trigg, M., Mdee, A., Carr, A., Bhave, A., Solano-Correa, Y. T.,  
469 Pencue-Fierro, E. L., Teferi, E., Haile, A. T., Yusop, Z., Alias, N. E., Sa'adi, Z., Bin  
470 Ramzan, M. A., Dhanya, C. T., & Shukla, P. (2022). The Role of Global Data Sets for  
471 Riverine Flood Risk Management at National Scales. *Water Resources Research*, 58(4).  
472 <https://doi.org/10.1029/2021wr031555>

473 Birkmann, J., & Welle, T. (2015). Assessing the risk of loss and damage: Exposure,  
474 vulnerability and risk to climate-related hazards for different country classifications.  
475 *International Journal of Global Warming*, 8(2), 191–212.  
476 <https://doi.org/10.1504/IJGW.2015.071963>

477 Boulange, J., Hanasaki, N., Yamazaki, D., & Pokhrel, Y. (2021). Role of dams in reducing  
478 global flood exposure under climate change. *Nature Communications*, 12(1).  
479 <https://doi.org/10.1038/s41467-020-20704-0>



- 480 Brown, J. D., & Heuvelink, G. B. M. (2005). Assessing Uncertainty Propagation through  
 481 Physically Based Models of Soil Water Flow and Solute Transport. *Encyclopedia of*  
 482 *Hydrological Sciences*. <https://doi.org/10.1002/0470848944.HSA081>
- 483 Chaudhari, S., & Pokhrel, Y. (2022). Alteration of River Flow and Flood Dynamics by Existing  
 484 and Planned Hydropower Dams in the Amazon River Basin. *Water Resources Research*,  
 485 58(5). <https://doi.org/10.1029/2021WR030555>
- 486 Cook, A., & Merwade, V. (2009). Effect of topographic data, geometric configuration and  
 487 modeling approach on flood inundation mapping. *Journal of Hydrology*, 377(1–2), 131–  
 488 142. <https://doi.org/10.1016/J.JHYDROL.2009.08.015>
- 489 Dang, H., Pokhrel, Y., Shin, S., Stelly, J., Ahlquist, D., & Du Bui, D. (2022). Hydrologic  
 490 balance and inundation dynamics of Southeast Asia’s largest inland lake altered by  
 491 hydropower dams in the Mekong River basin. *Science of The Total Environment*, 831,  
 492 154833. <https://doi.org/10.1016/J.SCITOTENV.2022.154833>
- 493 Dang, T. D., Chowdhury, A. K., & Galelli, S. (2019). On the representation of water reservoir  
 494 storage and operations in large-scale hydrological models: implications on model  
 495 parameterization and climate change impact assessments. *Hydrology and Earth System*  
 496 *Sciences Discussions*, 1–34. <https://doi.org/10.5194/hess-2019-334>
- 497 de Moel, H., Jongman, B., Kreibich, H., Merz, B., Penning-Rowsell, E., & Ward, P. J. (2015).  
 498 Flood risk assessments at different spatial scales. *Mitigation and Adaptation Strategies for*  
 499 *Global Change*, 20(6), 865–890. <https://doi.org/10.1007/s11027-015-9654-z>
- 500 Dey, S., Saksena, S., Winter, D., Merwade, V., & McMillan, S. (2022). Incorporating Network  
 501 Scale River Bathymetry to Improve Characterization of Fluvial Processes in Flood  
 502 Modeling. *Water Resources Research*, 58(11), e2020WR029521.  
 503 <https://doi.org/10.1029/2020WR029521>
- 504 Di Baldassarre, G., & Montanari, A. (2009). Uncertainty in river discharge observations: A  
 505 quantitative analysis. *Hydrology and Earth System Sciences*, 13(6), 913–921.  
 506 <https://doi.org/10.5194/HESS-13-913-2009>
- 507 Dottori, F., Salamon, P., Bianchi, A., Alfieri, L., Hirpa, F. A., & Feyen, L. (2016). Development  
 508 and evaluation of a framework for global flood hazard mapping. *Advances in Water*  
 509 *Resources*, 94, 87–102. <https://doi.org/10.1016/J.ADVWATRES.2016.05.002>
- 510 Eidsvig, U. M. K., Kristensen, K., & Vangelsten, B. V. (2017). Assessing the risk posed by  
 511 natural hazards to infrastructures. *Natural Hazards and Earth System Sciences*, 17(3), 481–  
 512 504. <https://doi.org/10.5194/nhess-17-481-2017>
- 513 Fredrick, O. (2017, May 19). Excavators allege debris was used to bury storey in Chhatar  
 514 Manzil. *Hindustan Times*. [https://www.hindustantimes.com/lucknow/excavators-allege-](https://www.hindustantimes.com/lucknow/excavators-allege-debris-was-used-to-bury-storey-in-chhatar-manzil/story-mMm8Dwog3azR6SSEmpvjIO.html)  
 515 [debris-was-used-to-bury-storey-in-chhatar-manzil/story-](https://www.hindustantimes.com/lucknow/excavators-allege-debris-was-used-to-bury-storey-in-chhatar-manzil/story-mMm8Dwog3azR6SSEmpvjIO.html)  
 516 [mMm8Dwog3azR6SSEmpvjIO.html](https://www.hindustantimes.com/lucknow/excavators-allege-debris-was-used-to-bury-storey-in-chhatar-manzil/story-mMm8Dwog3azR6SSEmpvjIO.html)
- 517 Gaur, A., & Gaur, A. (2018). *Future Changes in Flood Hazards across Canada under a*  
 518 *Changing Climate*. <https://doi.org/10.3390/w10101441>

- 519 Ghosh, A., & Kar, S. K. (2018). Application of analytical hierarchy process (AHP) for flood risk  
520 assessment: a case study in Malda district of West Bengal, India. *Natural Hazards*, 94(1),  
521 349–368. <https://doi.org/10.1007/s11069-018-3392-y>
- 522 Hanasaki, N., Kanae, S., Oki, T., Masuda, K., Motoya, K., Shirakawa, N., Shen, Y., & Tanaka,  
523 K. (2008). An integrated model for the assessment of global water resources - Part 1:  
524 Model description and input meteorological forcing. *Hydrology and Earth System  
525 Sciences*, 12(4), 1007–1025. <https://doi.org/10.5194/HESS-12-1007-2008>
- 526 Hanasaki, N., Yoshikawa, S., Pokhrel, Y., & Kanae, S. (2018). A global hydrological simulation  
527 to specify the sources of water used by humans. *Hydrology and Earth System Sciences*,  
528 22(1), 789–817. <https://doi.org/10.5194/hess-22-789-2018>
- 529 He, X., Bryant, B. P., Moran, T., Mach, K. J., Wei, Z., & Freyberg, D. L. (2021). Climate-  
530 informed hydrologic modeling and policy typology to guide managed aquifer recharge.  
531 *Science Advances*, 7(17), 6025–6046.  
532 [https://doi.org/10.1126/SCIADV.ABE6025/SUPPL\\_FILE/ABE6025\\_SM.PDF](https://doi.org/10.1126/SCIADV.ABE6025/SUPPL_FILE/ABE6025_SM.PDF)
- 533 Hirabayashi, Y., Mahendran, R., Koirala, S., Konoshima, L., Yamazaki, D., Watanabe, S., Kim,  
534 H., & Kanae, S. (2013). Global flood risk under climate change. *Nature Climate Change*,  
535 3(9), 816–821. <https://doi.org/10.1038/nclimate1911>
- 536 Hirabayashi, Y., Tanoue, M., Sasaki, O., Zhou, X., & Yamazaki, D. (2021). Global exposure to  
537 flooding from the new CMIP6 climate model projections. *Scientific Reports*, 0123456789,  
538 1–7. <https://doi.org/10.1038/s41598-021-83279-w>
- 539 Hochrainer-Stigler, S., Schinko, T., Hof, A., & Ward, P. J. (2021). Adaptive risk management  
540 strategies for governments under future climate and socioeconomic change: An application  
541 to riverine flood risk at the global level. *Environmental Science and Policy*, 125, 10–20.  
542 <https://doi.org/10.1016/j.envsci.2021.08.010>
- 543 Hooper, E., & Chapman, L. (2012). The impacts of climate change on national road and rail  
544 networks. In *Transport and Sustainability* (Vol. 2, pp. 105–136). Emerald Group  
545 Publishing Ltd. [https://doi.org/10.1108/S2044-9941\(2012\)0000002008](https://doi.org/10.1108/S2044-9941(2012)0000002008)
- 546 Hu, P., Zhang, Q., Shi, P., Chen, B., & Fang, J. (2018). Flood-induced mortality across the  
547 globe: Spatiotemporal pattern and influencing factors. *Science of The Total Environment*,  
548 643, 171–182. <https://doi.org/10.1016/J.SCITOTENV.2018.06.197>
- 549 IPCC. (2014). *Climate Change 2014: Synthesis Report. Contribution of Working Groups I, II,  
550 and III to the Fifth Assessment Report of the. Geneva, Switzerland: Intergovernmental  
551 Panel on Climate Change.*
- 552 Jain, G., Singh, C., Coelho, K., & Malladi, T. (2017). *Long-term implications of humanitarian  
553 responses The case of Chennai.*  
554 <http://pubs.iied.org/10840IIEDwww.iied.org@iiedwww.facebook.com/theIIED>
- 555 Joint Research Centre (JRC), European Commission and Center for International Earth Science  
556 Information Network (CIESIN), & Columbia University. (2021). *Global Human Settlement  
557 Layer: Population and Built-Up Estimates, and Degree of Urbanization Settlement Model*

- 558 *Grid. Palisades, NY: NASA Socioeconomic Data and Applications Center (SEDAC).*  
559 <https://doi.org/10.7927/h4154f0w>
- 560 Joshi, V. (2014, September 14). Have we learnt from past floods? Clearly not! *Hindustan Times*  
561 *(Lucknow)*. [https://www.pressreader.com/india/hindustan-times-](https://www.pressreader.com/india/hindustan-times-lucknow/20140914/281646778342401)  
562 [lucknow/20140914/281646778342401](https://www.pressreader.com/india/hindustan-times-lucknow/20140914/281646778342401)
- 563 Kalantari, Z., Briel, A., Lyon, S. W., Olofsson, B., & Folkesson, L. (2014). On the utilization of  
564 hydrological modelling for road drainage design under climate and land use change.  
565 *Science of the Total Environment*, 475, 97–103.  
566 <https://doi.org/10.1016/J.SCITOTENV.2013.12.114>
- 567 Kimuli, J. B., Di, B., Zhang, R., Wu, S., Li, J., & Yin, W. (2021). A multisource trend analysis  
568 of floods in Asia-Pacific 1990–2018: Implications for climate change in sustainable  
569 development goals. In *International Journal of Disaster Risk Reduction* (Vol. 59). Elsevier  
570 Ltd. <https://doi.org/10.1016/j.ijdr.2021.102237>
- 571 Koks, E. E., Rozenberg, J., Zorn, C., Tariverdi, M., Vousdoukas, M., Fraser, S. A., Hall, J. W.,  
572 & Hallegatte, S. (2019). A global multi-hazard risk analysis of road and railway  
573 infrastructure assets. *Nature Communications*, 10(1). [https://doi.org/10.1038/s41467-019-](https://doi.org/10.1038/s41467-019-10442-3)  
574 [10442-3](https://doi.org/10.1038/s41467-019-10442-3)
- 575 Kushwaha, A. P., Tiwari, A. D., Dangar, S., Shah, H., Mahto, S. S., & Mishra, V. (2021).  
576 Multimodel assessment of water budget in Indian sub-continental river basins. *Journal of*  
577 *Hydrology*, 603, 126977. <https://doi.org/10.1016/J.JHYDROL.2021.126977>
- 578 Laiolo, P., Gabellani, S., Campo, L., Cenci, L., Silvestro, F., Delogu, F., Boni, G., Rudari, R.,  
579 Puca, S., & Pisani, A. R. (2015). Assimilation of remote sensing observations into a  
580 continuous distributed hydrological model: Impacts on the hydrologic cycle. *International*  
581 *Geoscience and Remote Sensing Symposium (IGARSS), 2015-November*, 1308–1311.  
582 <https://doi.org/10.1109/IGARSS.2015.7326015>
- 583 Lehner, B., Liermann, C. R., Revenga, C., Vörösmarty, C., Fekete, B., Crouzet, P., Döll, P.,  
584 Endejan, M., Frenken, K., Magome, J., Nilsson, C., Robertson, J. C., Rödel, R., Sindorf,  
585 N., & Wisser, D. (2011). High-resolution mapping of the world's reservoirs and dams for  
586 sustainable river-flow management. In *Frontiers in Ecology and the Environment* (Vol. 9,  
587 Issue 9, pp. 494–502). <https://doi.org/10.1890/100125>
- 588 Marchand, M., Dahm, R., Buurman, J., Sethurathinam, S., & Sprengers, C. (2022). Flood  
589 protection by embankments in the Brahmani–Baitarani river basin, India: a risk-based  
590 approach. *International Journal of Water Resources Development*, 38(2), 242–261.  
591 <https://doi.org/10.1080/07900627.2021.1899899>
- 592 Mateo, C. M., Hanasaki, N., Komori, D., & Tanaka, K. (2014). Assessing the impacts of  
593 reservoir operation to floodplain inundation by combining hydrological, reservoir  
594 management, and hydrodynamic models. *AGU Publications*, 7245–7266.  
595 <https://doi.org/10.1002/2013WR014845>.Received
- 596 Mateo, C. M. R., Hanasaki, N., Komori, D., Yoshimura, K., Kiguchi, M., Champathong, A.,  
597 Yamazaki, D., Sukhapunphan, T., & Oki, T. (2013). A simulation study on modifying

- 598 reservoir operation rules: Tradeoffs between flood mitigation and water supply. *IAHS-*  
599 *AISH Proceedings and Reports*, 362(July), 33–40.
- 600 Mateo, C. M. R., Hanasaki, N., Komori, D., Yoshimura, K., Kiguchi, M., Champathong, A.,  
601 Yamazaki, D., Sukhapunphan, T., & Oki, T. (2014). Flood risk and climate change:  
602 global and regional perspectives. *Hydrological Sciences Journal*, 59(1), 1–28.  
603 <https://doi.org/10.1080/02626667.2013.857411>
- 604 Mishra, D. K. (2015, March 10). 1948 Floods in Bihar-2 Inaugural flood after Independence –  
605 Official Version of Floods and its Aftermath. *SANDRP*. [https://sandrp.in/2015/03/10/1948-](https://sandrp.in/2015/03/10/1948-floods-in-bihar-2-inaugural-flood-after-independence-official-version-of-floods-and-its-aftermath/)  
606 [floods-in-bihar-2-inaugural-flood-after-independence-official-version-of-floods-and-its-](https://sandrp.in/2015/03/10/1948-floods-in-bihar-2-inaugural-flood-after-independence-official-version-of-floods-and-its-aftermath/)  
607 [aftermath/](https://sandrp.in/2015/03/10/1948-floods-in-bihar-2-inaugural-flood-after-independence-official-version-of-floods-and-its-aftermath/)
- 608 Mishra, V., & Shah, H. L. (2018). Hydroclimatological Perspective of the Kerala Flood of 2018.  
609 *Journal of the Geological Society of India*, 92(5), 645–650. [https://doi.org/10.1007/s12594-](https://doi.org/10.1007/s12594-018-1079-3)  
610 [018-1079-3](https://doi.org/10.1007/s12594-018-1079-3)
- 611 Mishra, V., Tiwari, A. D., & Kumar, R. (2022). Warming climate and ENSO variability enhance  
612 the risk of sequential extremes in India. *One Earth*, 5(11), 1250–1259.  
613 <https://doi.org/10.1016/J.ONEEAR.2022.10.013>
- 614 Mittal, N., Bhave, A. G., Mishra, A., & Singh, R. (2016). Impact of human intervention and  
615 climate change on natural flow regime. *Water Resources Management*, 30(2), 685–699.  
616 <https://doi.org/10.1007/s11269-015-1185-6>
- 617 Mohanty, M. P., Mudgil, S., & Karmakar, S. (2020). Flood management in India: A focussed  
618 review on the current status and future challenges. In *International Journal of Disaster*  
619 *Risk Reduction* (Vol. 49). Elsevier Ltd. <https://doi.org/10.1016/j.ijdr.2020.101660>
- 620 Mohapatra, P. K., & Singh, R. D. (2003). Flood management in India. *Natural Hazards*, 28,  
621 131–143. <https://doi.org/10.1177/0019556120120109>
- 622 Mukherjee, S., Aadhar, S., Stone, D., & Mishra, V. (2018). Increase in extreme precipitation  
623 events under anthropogenic warming in India. *Weather and Climate Extremes*, 20, 45–53.  
624 <https://doi.org/10.1016/J.WACE.2018.03.005>
- 625 Nanditha, J. S., Kushwaha, A. P., Singh, R., Malik, I., Solanki, H., Singh Chupal, D., Dangar, S.,  
626 Shwarup Mahto, S., Mishra, V., Vegad, U., Chuphal, D. S., & Mahto, S. S. (2022). The  
627 Pakistan flood of August 2022: causes and implications. *Authorea Preprints*.  
628 <https://doi.org/10.1002/ESSOAR.10512560.1>
- 629 Nanditha, J. S., & Mishra, V. (2021). On the need of ensemble flood forecast in India. *Water*  
630 *Security*, 12, 100086. <https://doi.org/10.1016/J.WASEC.2021.100086>
- 631 Nanditha, J. S., & Mishra, V. (2022). Multiday Precipitation Is a Prominent Driver of Floods in  
632 Indian River Basins. *Water Resources Research*, 58(7), e2022WR032723.  
633 <https://doi.org/10.1029/2022WR032723>
- 634 Nilsson, C., Catherine, \*, Reidy, A., Dynesius, M., & Revenga, C. (2005). Fragmentation and  
635 Flow Regulation of the World's Large River Systems. In *SCIENCE* (Vol. 308).  
636 [www.sciencemag.org](http://www.sciencemag.org)

- 637 Padhra, A. (2022). Tourism in India and the Impact of Weather and Climate. In *Indian Tourism*  
638 (pp. 187–197). Emerald Publishing Limited. [https://doi.org/10.1108/978-1-80262-937-](https://doi.org/10.1108/978-1-80262-937-820221013)  
639 [820221013](https://doi.org/10.1108/978-1-80262-937-820221013)
- 640 Pai, D. S., Sridhar, L., Rajeevan, M., Sreejith, O. P., Satbhai, N. S., & Mukhopadhyay, B.  
641 (2014). Development of a new high spatial resolution ( $0.25^\circ \times 0.25^\circ$ ) long period (1901-  
642 2010) daily gridded rainfall data set over India and its comparison with existing data sets  
643 over the region. *Mausam*, *65*(1), 1–18.
- 644 Pathak, S., Liu, M., Jato-Espino, D., & Zevenbergen, C. (2020). Social, economic and  
645 environmental assessment of urban sub-catchment flood risks using a multi-criteria  
646 approach: A case study in Mumbai City, India. *Journal of Hydrology*, *591*, 125216.  
647 <https://doi.org/10.1016/J.JHYDROL.2020.125216>
- 648 Peduzzi, P., Dao, H., Herold, C., & Mouton, F. (2009). Natural Hazards and Earth System  
649 Sciences Assessing global exposure and vulnerability towards natural hazards: the Disaster  
650 Risk Index. In *Hazards Earth Syst. Sci* (Vol. 9). [www.nat-hazards-earth-syst-](http://www.nat-hazards-earth-syst-sci.net/9/1149/2009/)  
651 [sci.net/9/1149/2009/](http://www.nat-hazards-earth-syst-sci.net/9/1149/2009/)
- 652 Pekel, J. F., Cottam, A., Gorelick, N., & Belward, A. S. (2016). High-resolution mapping of  
653 global surface water and its long-term changes. *Nature*, *540*(7633), 418–422.  
654 <https://doi.org/10.1038/nature20584>
- 655 Pokhrel, Y., Shin, S., Lin, Z., Yamazaki, D., & Qi, J. (2018). Potential Disruption of Flood  
656 Dynamics in the Lower Mekong River Basin Due to Upstream Flow Regulation. *Scientific*  
657 *Reports*, *8*(1). <https://doi.org/10.1038/s41598-018-35823-4>
- 658 Poulin, A., Brissette, F., Leconte, R., Arsenault, R., & Malo, J. S. (2011). Uncertainty of  
659 hydrological modelling in climate change impact studies in a Canadian, snow-dominated  
660 river basin. *Journal of Hydrology*, *409*(3–4), 626–636.  
661 <https://doi.org/10.1016/J.JHYDROL.2011.08.057>
- 662 Rentschler, J., Salhab, M., & Jafino, B. A. (2022). Flood exposure and poverty in 188 countries.  
663 *Nature Communications*, *13*(1). <https://doi.org/10.1038/s41467-022-30727-4>
- 664 Roxy, M. K., Ghosh, S., Pathak, A., Athulya, R., Mujumdar, M., Murtugudde, R., Terray, P., &  
665 Rajeevan, M. (2017). A threefold rise in widespread extreme rain events over central India.  
666 *Nature Communications*, *8*(1). <https://doi.org/10.1038/s41467-017-00744-9>
- 667 Roy, B., Khan, M. S. M., Saiful Islam, A. K. M., Khan, M. J. U., & Mohammed, K. (2021).  
668 Integrated flood risk assessment of the arial khan river under changing climate using ipcc  
669 ar5 risk framework. *Journal of Water and Climate Change*, *12*(7), 3421–3447.  
670 <https://doi.org/10.2166/wcc.2021.341>
- 671 Shah, H. L., & Mishra, V. (2016). Hydrologic Changes in Indian Subcontinental River Basins  
672 (1901–2012). *Journal of Hydrometeorology*, *17*(10), 2667–2687.  
673 <https://doi.org/10.1175/JHM-D-15-0231.1>
- 674 Sheffield, J., Goteti, G., & Wood, E. F. (2006). *Development of a 50-Year High-Resolution*  
675 *Global Dataset of Meteorological Forcings for Land Surface Modeling*.

- 676 Singh, A., Mani, M., & Vishnoi, R. K. (2021). Tehri Dam—A Savior from Climate Change Led  
677 Extreme Events. *INCOLD Journal (A Half Yearly Technical Journal of Indian Committee*  
678 *on Large Dams)*, 10(2), 44–50.
- 679 Singh, P., Sinha, V. S. P., Vijhani, A., & Pahuja, N. (2018). Vulnerability assessment of urban  
680 road network from urban flood. *International Journal of Disaster Risk Reduction*, 28, 237–  
681 250. <https://doi.org/10.1016/J.IJDRR.2018.03.017>
- 682 Smith, A., Bates, P. D., Wing, O., Sampson, C., Quinn, N., & Neal, J. (2019). New estimates of  
683 flood exposure in developing countries using high-resolution population data. *Nature*  
684 *Communications*, 10(1). <https://doi.org/10.1038/s41467-019-09282-y>
- 685 Srivastava, A. K., Rajeevan, M., & Kshirsagar, S. R. (2009). Development of a high resolution  
686 daily gridded temperature data set ( 1969 – 2005 ) for the Indian region. *Atmospheric*  
687 *Science Letters*, 10(October), 249–254. <https://doi.org/10.1002/asl>
- 688 Stephens, E. M., Bates, P. D., Freer, J. E., & Mason, D. C. (2012). The impact of uncertainty in  
689 satellite data on the assessment of flood inundation models. *Journal of Hydrology*, 414–  
690 415, 162–173. <https://doi.org/10.1016/J.JHYDROL.2011.10.040>
- 691 Tanoue, M. (2020). *Future river-flood damage increases under aggressive adaptations*. 1–12.
- 692 Teng, J., Jakeman, A. J., Vaze, J., Croke, B. F. W., Dutta, D., & Kim, S. (2017). Flood  
693 inundation modelling: A review of methods, recent advances and uncertainty analysis.  
694 *Environmental Modelling & Software*, 90, 201–216.  
695 <https://doi.org/10.1016/J.ENVSOFT.2017.01.006>
- 696 UNISDR. (2011). *Global Assessment Report on Disaster Risk Reduction 2011, Revealing*  
697 *Risk, Redefining Development, United Nations International Strategy*  
698 *for Disaster Reduction Secretariat, Geneva, 2011.*  
699 [https://www.undp.org/publications/2011-global-assessment-report-disaster-risk-reduction?utm\\_source=EN&utm\\_medium=GSR&utm\\_content=US\\_UNDP\\_PaidSearch\\_Brand\\_English&utm\\_campaign=CENTRAL&c\\_src=CENTRAL&c\\_src2=GSR&gclid=CjwKCAiAqaWdBhAvEiwAGAqlttbTEIs1543d8ZuHyzCatyJutiZP2w2Wp41vZBSiouchJ7PvGpIcUBoCxOYQAvD\\_BwE](https://www.undp.org/publications/2011-global-assessment-report-disaster-risk-reduction?utm_source=EN&utm_medium=GSR&utm_content=US_UNDP_PaidSearch_Brand_English&utm_campaign=CENTRAL&c_src=CENTRAL&c_src2=GSR&gclid=CjwKCAiAqaWdBhAvEiwAGAqlttbTEIs1543d8ZuHyzCatyJutiZP2w2Wp41vZBSiouchJ7PvGpIcUBoCxOYQAvD_BwE)
- 700  
701  
702  
703
- 704 UNISDR. (2013). *Global Assessment Report on Disaster Risk Reduction 2013, From Shared*  
705 *Risk to Shared Value: the Business Case for Disaster Risk Reduction, United Nations*  
706 *International Strategy for Disaster Reduction Secretariat, Geneva, 2013.*  
707 <https://www.undrr.org/publication/global-assessment-report-disaster-risk-reduction-2013>
- 708 Varis, O., Taka, M., & Tortajada, C. (2022). Global human exposure to urban riverine floods  
709 and storms. *River*. <https://doi.org/10.1002/rvr.2.1>
- 710 Vu, D. T., Dang, T. D., Galelli, S., & Hossain, F. (2022). Satellite observations reveal 13 years  
711 of reservoir filling strategies, operating rules, and hydrological alterations in the Upper  
712 Mekong River basin. *Hydrology and Earth System Sciences*, 26(9), 2345–2364.  
713 <https://doi.org/10.5194/hess-26-2345-2022>
- 714 Ward, P. J., Jongman, B., Weiland, F. S., Bouwman, A., Van Beek, R., Bierkens, M. F. P.,  
715 Ligtoet, W., & Winsemius, H. C. (2013). Assessing flood risk at the global scale: Model

716 setup, results, and sensitivity. *Environmental Research Letters*, 8(4).  
717 <https://doi.org/10.1088/1748-9326/8/4/044019>

718 Winsemius, H. C., Jongman, B., Veldkamp, T. I. E., Hallegatte, S., Bangalore, M., & Ward, P. J.  
719 (2018). Disaster risk, climate change, and poverty: Assessing the global exposure of poor  
720 people to floods and droughts. *Environment and Development Economics*, 23(3), 328–348.  
721 <https://doi.org/10.1017/S1355770X17000444>

722 Winsemius, H. C., van Beek, L. P. H., Jongman, B., Ward, P. J., & Bouwman, A. (2013). A  
723 framework for global river flood risk assessments. *Hydrology and Earth System Sciences*,  
724 17(5), 1871–1892. <https://doi.org/10.5194/hess-17-1871-2013>

725 Yamazaki, D., De Almeida, G. A. M., & Bates, P. D. (2013). Improving computational  
726 efficiency in global river models by implementing the local inertial flow equation and a  
727 vector-based river network map. *Water Resources Research*, 49(11), 7221–7235.  
728 <https://doi.org/10.1002/wrcr.20552>

729 Yamazaki, D., Kanae, S., Kim, H., & Oki, T. (2011). *A physically based description of*  
730 *floodplain inundation dynamics in a global river routing model*. 47(February), 1–21.  
731 <https://doi.org/10.1029/2010WR009726>

732 Yamazaki, D., Watanabe, S., & Hirabayashi, Y. (2018). Global Flood Risk Modeling and  
733 Projections of Climate Change Impacts. *Global Flood Hazard: Applications in Modeling,*  
734 *Mapping, and Forecasting*, 233, 185–203. <http://cmip-pcmdi.llnl.gov/>

735 Yang, T., Sun, F., Gentine, P., Liu, W., Wang, H., Yin, J., Du, M., & Liu, C. (2019). Evaluation  
736 and machine learning improvement of global hydrological model-based flood simulations.  
737 *Environmental Research Letters*, 14(11). <https://doi.org/10.1088/1748-9326/ab4d5e>

738 Zajac, Z., Revilla-Romero, B., Salamon, P., Burek, P., Hirpa, F., & Beck, H. (2017). The impact  
739 of lake and reservoir parameterization on global streamflow simulation. *Journal of*  
740 *Hydrology*, 548, 552–568. <https://doi.org/10.1016/j.jhydrol.2017.03.022>

741 Zhao, F., Veldkamp, T. I. E., Frieler, K., Schewe, J., Ostberg, S., Willner, S., Schauburger, B.,  
742 Gosling, S. N., Schmied, H. M., Portmann, F. T., Leng, G., Huang, M., Liu, X., Tang, Q.,  
743 Hanasaki, N., Biemans, H., Gerten, D., Satoh, Y., Pokhrel, Y., ... Yamazaki, D. (2017).  
744 The critical role of the routing scheme in simulating peak river discharge in global  
745 hydrological models. *Environmental Research Letters*, 12(7). [https://doi.org/10.1088/1748-](https://doi.org/10.1088/1748-9326/aa7250)  
746 [9326/aa7250](https://doi.org/10.1088/1748-9326/aa7250)

747